

Spatiotemporal dynamics in a diffusive ratio-dependent predator–prey model near a Hopf–Turing bifurcation point

Yongli Song^{a,*}, Xingfu Zou^b

^a Department of Mathematics, Tongji University, Shanghai 200092, PR China

^b Department of Applied Mathematics, University of Western Ontario, London, Ontario N6A 5B7, Canada

ARTICLE INFO

Article history:

Received 19 November 2013

Received in revised form 8 March 2014

Accepted 21 April 2014

Available online 9 May 2014

Keywords:

Pattern formation

Normal form

Dynamical classification

Steady state

Periodic solution

ABSTRACT

Spatiotemporal dynamics in a ratio-dependent predator–prey model with diffusion is studied by analytical methods. Normal forms associated with codimension-two Hopf–Turing bifurcation are derived, which can be used to understand and classify the spatiotemporal dynamics of the model for values of parameters close to the Hopf–Turing bifurcation point. In the vicinity of this degenerate point, a wealth of complex spatiotemporal dynamics are observed. Our theoretical results are confirmed by numerical simulations.

© 2014 Elsevier Ltd. All rights reserved.

1. Introduction

After the pioneering works of Lotka and Volterra, the qualitative research on the dynamics of predator–prey models has been in the focus of ecological and mathematical sciences (see, e.g., Freedman [1], Murray [2] and references therein). Predator–prey systems are characterized by the interaction between species and their natural environments. Functional response is proposed for modeling predator–prey interactions, which describes how the consumption rate of individual consumers changes with respect to resource density. Traditionally, the functional response depends only on prey density and is called a prey-dependent functional response. Following Holling [3], the prey-dependent functional responses are generally classified into three types, which are called Holling's type I, II and III. The qualitative study on the prey-dependent predator–prey models is useful to help population ecologists understand the factors that influence population dynamics and has been regarded as important contributions that mathematics had for ecology.

However, the prey-dependent predator–prey models are very controversial among ecologists up to this day because of the following reasons: (1) it cannot explain the laboratory experiments and observations that the predators or both the predators and prey can either go extinction or coexist in oscillatory modes depending on the initial population densities (see [4–8]); (2) it exhibits the well known ‘paradox of enrichment’ formulated by Hairston et al. [9] and Rosenzweig [10], which states that enriching a predator–prey system (increasing the carrying capacity) will cause an increase in the equilibrium density of the predator but not in that of the prey, and will finally destabilize the positive equilibrium; (3) it exhibits the so-called ‘biological control paradox’ [11], which states that we cannot have a low and stable prey equilibrium density compared with its carrying capacity.

* Corresponding author.

E-mail address: 05143@tongji.edu.cn (Y. Song).

Recently, there are growing explicit biological and physiological evidences that when resources are scarce relative to predator density and predators have to search for food, the predator’s per-capita growth rate should decline with its density [6,5,12,13]. Thus, to overcome the disadvantages of the prey-dependent predator–prey models and to fit the recent laboratory experiments and observations, Arditi and Ginzburg [4] have suggested that a more suitable predator–prey theory should be based on the so-called ratio-dependent theory, which can be roughly stated as that the per capita predator growth rate should be a function of the ratio of prey to predator abundance. Based on the Holling type II function, they proposed the following ratio-dependent predator–prey model

$$\begin{aligned} \frac{dN}{dt} &= rN \left(1 - \frac{N}{K} \right) - \frac{\alpha NP}{P + \alpha \beta N}, \\ \frac{dP}{dt} &= \frac{\eta \alpha NP}{P + \alpha \beta N} - \gamma P, \end{aligned} \tag{1.1}$$

where N, P stand for prey and predator densities, respectively, and $r, K, \alpha, \beta, \eta, \gamma$ are positive constants that represent prey intrinsic growth rate, environmental carrying capacity, total attack rate for predator, handling time, conversion rate and predator death rate, respectively. System (1.1) and its more general version have been widely studied by many authors and these studies have shown that such models exhibit much richer dynamics than the traditional prey-dependent predator–prey model (see, for example, [14–22] and references therein). The effects of discrete and distributed delays on dynamics of the ratio-dependent predator–prey model have also been investigated by many researchers [23–26].

In reality, the species are distributed over space and interact each other within their spatial domain. The importance of spatial models has been recognized by the biologists for a long time and have been one of the dominant themes in both ecology and mathematical ecology due to its universal existence and importance [27–29,2]. In this paper, we consider the ratio-dependent predator–prey model (1.1) with diffusion. For simplicity, scaling the variables by $u = \alpha \beta N / (\eta K), v = \alpha \beta P / (\eta^2 K), \tilde{t} = \eta t / \beta$ and then dropping the tilde, the diffusive version of system (1.1) with Neumann boundary condition can be taken as the following reaction–diffusion system

$$\begin{cases} \frac{\partial u(x, t)}{\partial t} = d_1 \Delta u(x, t) + au(x, t) \left(1 - \frac{u(x, t)}{b} \right) - \frac{bu(x, t)v(x, t)}{bu(x, t) + v(x, t)}, \\ \frac{\partial v(x, t)}{\partial t} = d_2 \Delta v(x, t) + \left(\frac{bu(x, t)}{bu(x, t) + v(x, t)} - c \right) v(x, t), \\ u_x(0, t) = u_x(\pi, t) = v_x(0, t) = v_x(\pi, t) = 0, \quad t \geq 0, \\ u(x, t) = \phi(x, 0), \quad v(x, t) = \psi(x, 0) \geq 0 (\neq 0), \quad x \in [0, \pi], \end{cases} \tag{1.2}$$

where d_1 and d_2 are the diffusion coefficients for the prey and the predator, respectively.

Here we choose the closed interval $[0, \pi]$ as the spatial domain mainly for simplicity of notations in computing the normal forms and for convenience of carrying out demonstrating numeric results. General closed interval $[a, b]$ can be transformed to $[0, \pi]$ by a translation and rescaling. The choice of the homogeneous Neumann boundary condition accounts for a scenario that the spatial habitat is isolated from the outside (islands and lakes/ponds are such habitats), and thus there is no population flux on the boundary. In reality, there may be a situation in which the boundary is hostile and hence no individuals would choose to leave there, meaning that the homogeneous Dirichlet boundary condition should be posed on the boundary. For this case, there is no positive constant steady state. In this paper, we are only interested in the bifurcations from the positive constant steady state, corresponding to the homogeneous Neumann boundary condition.

The local and global stability of the unique positive constant equilibrium, Turing instability, dissipation, persistence as well as the existence of non-constant positive steady states of system (1.2) or similar systems have been studied in [30–33]. Spatiotemporal complexity, self-organized spatial patterns and chaos in the ratio-dependent predator–prey system have also been reported in [34–36] by numerical analysis.

The past investigations have revealed that spatial inhomogeneities can have an important impact on the dynamics of ecological populations [37–39]. This spatial inhomogeneity leads to a reaction–diffusion system, which can be used to describe how the movement of individuals in the domain and has been shown that such systems are capable of self-organized pattern formation (see, e.g., [40,41] and references therein). In the last decade, the focus of research has been shifted from the study of the formation of stationary spatial patterns induced by Turing instabilities to the study of the formation of spatio-temporal patterns. The dynamical system method is an efficient technology to theoretically understand the mechanisms of the formation of spatio-temporal patterns. Bifurcations of spatially homogeneous and inhomogeneous periodic solutions as well as nonconstant steady state solutions in predator–prey systems with diffusion have been recently studied by many researchers (see [42–47] and references therein). However, most of these work investigate the codimension-one Hopf bifurcation or steady-state bifurcation, where purely spatially or temporarily periodic pattern occurs. Interactions of the Hopf and steady-state bifurcations may bring about mixed spatiotemporal periodic patterns, domain structures displaying bistability between spatial and temporal modes, and space–time chaos. Although there is a large body of previous work on Hopf–Turing bifurcations of predator–prey type reaction–diffusion systems, with different levels of details and the rich dynamics near the bifurcation point were reported (see, for example [40,48–50] and references therein),

most of them are based on the numerical results but lack of the strictly theoretical analysis for the rich dynamics near this kind of bifurcation point. In this paper, we study the bifurcation scenarios near a codimension-two Hopf–Turing bifurcation point. The classification of the spatiotemporal dynamics in a neighborhood of the bifurcation point can be figured out in the framework of the normal forms.

The rest of the paper is organized as follows. In Section 2, the normal form for Hopf–Turing bifurcation is derived. In Section 3, the dynamics of the normal form and the corresponding spatiotemporal dynamics are investigated, and the analytic results are confirmed by numerical simulations. We conclude with a summary and a discussion of the results in Section 4.

2. Existence of the Hopf–Turing bifurcation

Clearly, the positive constant equilibrium $E^* = (u^*, v^*)$ with

$$u^* = \frac{b(a + (c - 1)b)}{a} > 0, \quad v^* = \frac{b^2(1 - c)(a + (c - 1)b)}{ac} > 0,$$

exists if and only if the following condition holds

(P0) $0 < c < 1, \quad a > b(1 - c).$

For the biological meaning, in the following, we always assume that the condition (P0) holds.

The linearization of (1.2) at the equilibrium E^* is

$$\begin{pmatrix} \frac{\partial u}{\partial t} \\ \frac{\partial v}{\partial t} \end{pmatrix} = d\Delta \begin{pmatrix} u \\ v \end{pmatrix} + A \begin{pmatrix} u \\ v \end{pmatrix}, \tag{2.1}$$

with

$$d\Delta = \begin{pmatrix} d_1\Delta & 0 \\ 0 & d_2\Delta \end{pmatrix}, \quad A = \begin{pmatrix} b(1 - c^2) - a & -c^2 \\ b(1 - c)^2 & c(c - 1) \end{pmatrix}.$$

For the Neumann boundary condition, define the real-valued Sobolev space

$$X = \left\{ (u, v)^T \in W^{2,2}(0, \pi), \frac{\partial u}{\partial x} = \frac{\partial v}{\partial x} = 0 \text{ at } x = 0, \pi \right\}.$$

It is well known that the eigenvalues of $d\Delta$ on X are $-d_1k^2$ and $-d_2k^2$, $k \in \mathbb{N}_0 = \{0, 1, 2, \dots\}$, with corresponding normalized eigenfunctions β_k^1 and β_k^2 , where

$$\beta_k^1(x) = \begin{pmatrix} \gamma_k(x) \\ 0 \end{pmatrix}, \quad \beta_k^2(x) = \begin{pmatrix} 0 \\ \gamma_k(x) \end{pmatrix}, \quad \gamma_k(x) = \frac{\cos(kx)}{\|\cos(kx)\|_{2,2}}, \quad k \in \mathbb{N}_0.$$

Then the normalized eigenfunctions form a normalized orthogonal basis for X . The linear stability of the positive equilibrium E^* can be analyzed by introducing a small inhomogeneous perturbation to the system (2.1) at the zero equilibrium. The perturbation solution of system (2.1) can be written as a spectral decomposition given by

$$\begin{pmatrix} u \\ v \end{pmatrix} = \sum_{k=0}^{\infty} q_k^T \begin{pmatrix} \beta_k^1 \\ \beta_k^2 \end{pmatrix} e^{\lambda_k t}, \quad q_k = \begin{pmatrix} q_{k1} \\ q_{k2} \end{pmatrix} \in \mathbb{C}^2, \tag{2.2}$$

where the spatial part is governed by the wave modes k and the temporal part by the corresponding eigenvalues λ describing the growth of the perturbation and then determining the stability of the equilibrium E^* . Substituting (2.2) into (2.1) yields the following characteristic equations

$$\Delta_k = \lambda^2 + T_k\lambda + J_k = 0, \tag{2.3}$$

where $k \in \mathbb{N}_0 \triangleq \{0, 1, 2, \dots\}$ and

$$T_k = (d_1 + d_2)k^2 - b(1 - c^2) + a + c(1 - c), \tag{2.4}$$

$$J_k = d_1d_2k^4 - (d_1c(c - 1) + d_2(b(1 - c^2) - a))k^2 + c(1 - c)(a + b(c - 1)). \tag{2.5}$$

We call the bifurcation a Hopf–Turing bifurcation if there exist a nonnegative integer k and a positive integer $n \neq k$ such that $\Delta_k = 0$ has a pair of purely imaginary roots and $\Delta_n = 0$ has a simple zero root, and no other roots of the characteristic equation (2.3) have zero real parts, and the transversality condition holds. The characteristic equation (2.3) has been studied in detail in [47]. In the following, we summarize some related results from [47] for the Hopf–Turing bifurcation analysis.

It follows from the assumption (P0) that in the absence of diffusion ($d_1, d_2 = 0$), the equilibrium E^* is asymptotically stable if and only if $a > b(1 - c^2) + c(c - 1)$, and $\Delta_0 = 0$ has a pair of purely imaginary roots $\pm\sqrt{J_0}i$ if and only if

$$a = b(1 - c^2) + c(c - 1), \quad b > 1, \tag{2.6}$$

at which system (1.2) undergoes a Hopf bifurcation near the equilibrium E^* . For fixed c , denote this Hopf bifurcation straight line in the b – a plane by H_0 .

Solving $J_k = 0$ for b , we have

$$a = a_T(k, b) \triangleq \frac{d_2(1 - c^2)k^2 + c(1 - c)^2}{d_2k^2 + c(1 - c)}b - \frac{d_1d_2k^4 + d_1c(1 - c)k^2}{d_2k^2 + c(1 - c)}. \tag{2.7}$$

Then the Turing bifurcation curve ℓ is formed by a sequence of line segments ℓ_k ($k = 1, 2, \dots$), where

$$\ell_k : a = a_T(k, b), \quad \text{for } b_{k-1} < b \leq b_k, \tag{2.8}$$

where b_k is determined by solving $a_T(k + 1, b) - a_T(k, b) = 0$ for b and defined by

$$b_k = \frac{d_1}{d_2} + \frac{k^2 + (k + 1)^2}{c(1 - c)}d_1 + \frac{k^2(k + 1)^2}{c^2(1 - c)^2}d_1d_2.$$

By (2.6)–(2.8), we can see that H_0 intersects with the straight line $a = b(1 - c)$ at $b = 1$ and the slope of the line segment ℓ_k is less than that of the Hopf bifurcation line H_0 , and that the straight line ℓ_1 intersects with the straight line $a = b(1 - c)$ at

$$b = b_0 \triangleq \frac{d_1}{d_2} + \frac{d_1}{c(1 - c)}. \tag{2.9}$$

By (2.9), it is easy to verify that $b_0 \geq 1$ is equivalent to

$$d_1 \geq d_1^*(c, d_2) \triangleq \frac{c(1 - c)}{d_2 + c(1 - c)}d_2.$$

This implies that the diffusion does not induce the Turing instability if $d_1 \geq d_1^*(c, d_2)$.

Combining (2.6) and (2.7) yields

$$b = b_{HT}(k) = -\frac{d_1d_2}{c^2(1 - c)^2}k^4 - \frac{d_1 - d_2}{c(1 - c)}k^2 + 1.$$

Noticing the fact that k is a nonnegative integer, $b_{HT}(k)$ has a maximum at $k = n$ with

$$n = \left\lceil \sqrt{\frac{(d_2 - d_1)c(1 - c)}{2d_1d_2}} \right\rceil, \tag{2.10}$$

where $\lceil \cdot \rceil$ is the integral function. From (2.7) and (2.8), we can conclude that the Hopf line H_0 intersects with the line segment ℓ_n at $b = b_{HT}(n)$. For simplification of notations, denote $b_{HT}(n)$ by b^* . Substituting $b = b^*$ into (2.6), we have $a = a^* \triangleq (1 - c^2)b^* + c(c - 1)$.

According to the above discussion and the qualitative theory of the dynamical system, the following results can be obtained.

Theorem 2.1. Assume that $0 < c < 1$, $a > b(1 - c)$, $0 < d_1 < d_1^*(c, d_2)$, H_0 and ℓ_n are defined by (2.6) and (2.8) with n defined by (2.10), respectively.

- (i) The Hopf bifurcation line H_0 intersects with the line segments ℓ_n and a codimension-2 Turing–Hopf bifurcation occurs at the intersect point (b^*, a^*) , where

$$b^* = -\frac{d_1d_2}{c^2(1 - c)^2}n^4 - \frac{d_1 - d_2}{c(1 - c)}n^2 + 1,$$

$$a^* = (1 - c^2)b^* + c(c - 1).$$

(ii) For $(b, a) = (b^*, a^*)$, the equation $\Delta_0 = 0$ has a pair of purely imaginary roots $\pm i\omega_c$ and $\Delta_n = 0$ has a simple zero root, and for Eq. (2.3), there are no other roots with zero real parts, where

$$\omega_c = \sqrt{c(1-c)(a^* + b^*(c-1))}.$$

3. Normal form on the center manifold for Hopf–Turing bifurcation

In the following, we employ the similar method as in [51] to compute the normal form on the center manifold associated with codimension-2 Hopf–Turing bifurcation such that the spatiotemporal dynamics of system (1.2) can be determined in the neighborhood of Hopf–Turing bifurcation point.

Introduce a new parameter $\mu \in \mathbb{R}$ by setting $\mu_1 = b - b^*$, $\mu_2 = a - a^*$ such that $\mu = 0$ is the value of Hopf–Turing bifurcation. Rewrite the positive equilibrium as a parameter-dependent form $E_\mu^*(u^*(\mu), v^*(\mu))$ with

$$u^*(\mu) = \frac{(b^* + \mu_1)(a^* + \mu_2 + (c-1)(b^* + \mu_1))}{a^* + \mu_2},$$

$$v^*(\mu) = \frac{(b^* + \mu_1)^2(1-c)(a^* + \mu_2 + (c-1)(b^* + \mu_1))}{(a^* + \mu_2)c}.$$

Setting $\tilde{u}(\cdot, t) = u(\cdot, t) - u^*(\mu)$, $\tilde{v}(\cdot, t) = v(\cdot, t) - v^*(\mu)$, $\tilde{U}(t) = (\tilde{u}(\cdot, t), \tilde{v}(\cdot, t))$ and then dropping the tildes for simplification of notation, system (1.2) can be written as the equation

$$\frac{\partial U}{\partial t} = d\Delta U + L_0(U) + f(U, \mu), \tag{3.1}$$

where

$$d\Delta u = \begin{pmatrix} d_1 \Delta u \\ d_2 \Delta v \end{pmatrix}, \quad L_0(U) = \begin{pmatrix} (b^*(1-c^2) - a^*)u - c^2v \\ b^*(1-c)^2u - c(1-c)v \end{pmatrix},$$

$$f(U, \mu) = \sum_{i+j+\ell_1+\ell_2 \geq 2} \frac{1}{i!j!\ell_1!\ell_2!} f_{ij\ell_1\ell_2} u^i v^j \mu_1^{\ell_1} \mu_2^{\ell_2}, \quad f_{ij\ell_1\ell_2} = (f_{ij\ell_1\ell_2}^{(1)}, f_{ij\ell_1\ell_2}^{(2)})^T,$$

with $f_{ij\ell_1\ell_2}^{(k)} = \frac{\partial^{i+j+\ell_1+\ell_2} \tilde{f}^{(n)}(0,0,0)}{\partial u^i \partial v^j \partial \mu_1^{\ell_1} \partial \mu_2^{\ell_2}}$, $k = 1, 2$, and

$$\tilde{f}^{(1)}(u, v, \mu_1, \mu_2) = (a^* + \mu_2)(u + u^*(\mu)) \left(1 - \frac{(u + u^*(\mu))}{(b^* + \mu_1)} \right) - \frac{(b^* + \mu_1)(u + u^*(\mu))(v + v^*(\mu))}{(b^* + \mu_1)(u + u^*(\mu)) + (v + v^*(\mu))},$$

$$\tilde{f}^{(2)}(u, v, \mu_1, \mu_2) = \frac{(b^* + \mu_1)(u + u^*(\mu))(v + v^*(\mu))}{(b^* + \mu_1)(u + u^*(\mu)) + (v + v^*(\mu))} - c(v + v^*(\mu)).$$

The linearized system of equation (3.1) at the origin is

$$\frac{\partial U}{\partial t} = \mathcal{L}(U). \tag{3.3}$$

Denote by $\Lambda = \{i\omega_c, -i\omega_c, 0\}$ the finite set of all eigenvalues of the linearized system (3.3) having zero real parts, with which a stable invariant manifold is associated. Set $\mathcal{B}_k = \text{span} \{[\varphi(\cdot), \beta_k^i] \beta_k^i \mid \varphi \in X, i = 1, 2\}$. Then it is easy to verify that

$$L_0(\mathcal{B}_k) \subset \text{span} \{\beta_k^1, \beta_k^2\}, \quad k \in \mathbb{N}_0.$$

Assume that $y(t) \in \mathbb{R}^2$ and

$$y^T(t) \begin{pmatrix} \beta_k^1 \\ \beta_k^2 \end{pmatrix} \in \mathcal{B}_k.$$

Then, on \mathcal{B}_k , the linear partial differential equation (3.3) is equivalent to the ODE on \mathbb{R}^2

$$\dot{y}(t) = \begin{pmatrix} -d_1 k^2 & 0 \\ 0 & -d_2 k^2 \end{pmatrix} y(t) + L_0(y(t)), \tag{3.4}$$

where for $y(t) \in \mathbb{R}^2$, we use the same formal expression $L_0(y(t))$ as in (3.2). Clearly, the linear ordinary differential equation (3.4) has the same characteristic equation (2.3) as the linear partial differential equation (3.3).

Let

$$\mathcal{M}_k = \begin{pmatrix} -d_1 k^2 + b^* (1 - c^2) - a^* & -c^2 \\ b^* (1 - c)^2 & -d_2 k^2 - c(1 - c) \end{pmatrix}, \tag{3.5}$$

be the characteristic matrix of Eq. (3.4). Then Λ is the finite set of all eigenvalues of the matrix (3.5) having zero real parts. The standard adjoint theory for ODEs can be used to decompose \mathbb{C}^2 by Λ as

$$\mathbb{C}^2 = P_k \oplus Q_k,$$

where P_k is the generalized eigenspace associated with the eigenvalues in Λ and $Q_k = \{\varphi \in \mathbb{C}^2 : \langle \psi, \varphi \rangle \text{ for all } \psi \in P_k^*\}$, where P_k^* is the dual space of P_k and $\langle \cdot, \cdot \rangle$ is the scalar product of two complex vectors defined by

$$\langle \psi^T, \varphi \rangle = \psi^T \varphi, \quad \text{for } \varphi, \psi \in \mathbb{C}^2$$

such that for dual bases Φ_k and Ψ_k of P_k and P_k^* , respectively, $\langle \Psi_k, \Phi_k \rangle = I_{m_k}$, where $m_k = \dim P_k$ and I_{m_k} is a $m_k \times m_k$ identity matrix.

For $U_1 = (u_1, v_1)^T, U_2 = (u_2, v_2)^T \in X$, define the inner product

$$[U_1, U_2] = \int_0^\pi (u_1 u_2 + v_1 v_2) dx$$

such that X becomes a Hilbert space.

Notice that $k = 0, n > 0$ in the Hopf–Turing bifurcation. By a straightforward calculation, we obtain $\Phi_0 = (p_0, \bar{p}_0), \Phi_n = p_n, \Psi_0 = \text{col} \left(\bar{q}_0^T, q_0^T \right), \Psi_n = q_n^T$, where

$$p_0 = \begin{pmatrix} 1 \\ \frac{b_* (1 - c^2) - a_* - i\omega_c}{c^2} \end{pmatrix}, \quad q_0 = \begin{pmatrix} \frac{c(1 - c) + i\omega_c}{2i\omega_k} \\ -\frac{c^2}{2i\omega_c} \end{pmatrix},$$

$$p_n = \begin{pmatrix} 1 \\ -\frac{d_1 n^2 - b_* (1 - c^2) + a_*}{c^2} \end{pmatrix}, \quad q_n = \begin{pmatrix} \frac{d_2 n^2 + c(1 - c)}{T_n} \\ -\frac{c^2}{T_n} \end{pmatrix}.$$

Using the above decomposition, the phase space X can be decomposed as

$$X = X^c \oplus X^s, \quad X^c = \text{Im} \pi, \quad X^s = \text{Ker} \pi, \tag{3.6}$$

where $\dim X^c = 3$, and $\pi : X \rightarrow X^c$ is the projection defined by

$$\pi(\varphi) = \left((p_0, \bar{p}_0) \left\langle \left(\begin{matrix} q_0^T \\ \bar{q}_0^T \end{matrix} \right), \left(\begin{matrix} [\varphi, \beta_0^1] \\ [\varphi, \beta_0^2] \end{matrix} \right) \right\rangle \right)^T \begin{pmatrix} \beta_0^1 \\ \beta_0^2 \end{pmatrix} + \left(p_n \left\langle q_n^T, \left(\begin{matrix} [\varphi, \beta_n^1] \\ [\varphi, \beta_n^2] \end{matrix} \right) \right\rangle \right)^T \begin{pmatrix} \beta_n^1 \\ \beta_n^2 \end{pmatrix}.$$

According to (3.6), $U = (u, v)^T \in X$ can be decomposed as

$$\begin{pmatrix} u \\ v \end{pmatrix} = \left(\Phi_0 \begin{pmatrix} z_1 \\ z_2 \end{pmatrix} \right)^T \begin{pmatrix} \beta_0^1 \\ \beta_0^2 \end{pmatrix} + (z_3 \Phi_n)^T \begin{pmatrix} \beta_n^1 \\ \beta_n^2 \end{pmatrix} + w$$

$$= (z_1 p_0 + z_2 \bar{p}_0) \gamma_0(x) + z_3 p_n \gamma_n(x) + \begin{pmatrix} w_1 \\ w_2 \end{pmatrix}, \tag{3.7}$$

where $z_1, z_2, z_3 \in \mathbb{R}, w \in X^s$. For simplicity of notations, in the rest of this section, we write

$$\begin{pmatrix} [f, \beta_\varsigma^1] \\ [f, \beta_\varsigma^2] \end{pmatrix}_{\varsigma=0}^{\varsigma=n}$$

for

$$\left(\left(\begin{matrix} [f, \beta_0^1] \\ [f, \beta_0^2] \end{matrix} \right), \left(\begin{matrix} [f, \beta_n^1] \\ [f, \beta_n^2] \end{matrix} \right) \right)^T.$$

Then, system (3.1) is equivalent to the following system

$$\begin{cases} \dot{z} = Bz + \Psi \left(\begin{matrix} [f(z, w, \mu), \beta_\zeta^1] \\ [f(z, w, \mu), \beta_\zeta^2] \end{matrix} \right)_{\zeta=0}^{\zeta=n} \\ \dot{w} = \mathcal{L}(w) + H(z, w, \mu), \end{cases} \tag{3.8}$$

where $B = \text{diag}\{i\omega_c, -i\omega_c, 0\}$, $\Psi = \text{diag}\{\Psi_0, \Psi_n\}$,

$$f(z, w, \mu) = f \left((z_1 p_0 + z_2 \bar{p}_0) \gamma_0(x) + z_3 p_n \gamma_n(x) + \begin{pmatrix} w_1 \\ w_2 \end{pmatrix}, \mu \right) \tag{3.9}$$

and

$$\begin{aligned} H(z, w, \mu) = & f(z, w, \mu) - \left(\left\langle \bar{q}_0^T, \begin{pmatrix} [f(z, w, \mu), \beta_0^1] \\ [f(z, w, \mu), \beta_0^2] \end{pmatrix} \right\rangle p_0 \right. \\ & \left. + \left\langle \bar{q}_0^T, \begin{pmatrix} [f(z, w, \mu), \beta_0^1] \\ [f(z, w, \mu), \beta_0^2] \end{pmatrix} \right\rangle \bar{p}_0 \right) \gamma_0(x) - \left\langle \bar{q}_n^T, \begin{pmatrix} [f(z, w, \mu), \beta_n^1] \\ [f(z, w, \mu), \beta_n^2] \end{pmatrix} \right\rangle p_n \gamma_n(x). \end{aligned} \tag{3.10}$$

Consider the formal Taylor expansion

$$f(\varphi, \mu) = \sum_{j \geq 2} \frac{1}{j!} f_j(\varphi, \mu),$$

where f_j is the j th Fréchet derivative of f . Then (3.8) is written as

$$\begin{cases} \dot{z} = Bz + \sum_{j \geq 2} \frac{1}{j!} f_j^1(z, w, \mu), \\ \dot{w} = \mathcal{L}(w) + \sum_{j \geq 2} \frac{1}{j!} f_j^2(z, w, \mu), \end{cases} \tag{3.11}$$

where

$$f_j^1(z, w, \mu) = \Psi \left(\begin{matrix} [f_j(z, w, \mu), \beta_\zeta^1] \\ [f_j(z, w, \mu), \beta_\zeta^2] \end{matrix} \right)_{\zeta=0}^{\zeta=n}, \quad f_j^2(z, w, \mu) = H_j(z, w, \mu). \tag{3.12}$$

As for autonomous ODEs in the finite dimension space [52], by a recursive transformation of variables

$$(z, w) = (\tilde{z}, \tilde{w}) + \frac{1}{j!} (U_j^1(\tilde{z}, \mu), U_j^2(\tilde{z}, \mu)), \quad j \geq 2,$$

where U_j^1 and U_j^2 are homogeneous polynomials of degree j in \tilde{z} and μ , and for simplification of notation, dropping the tilde after each transformation of variable, then the normal form on the center manifold for (3.8) (or (3.11)) is

$$\dot{z} = Bz + \frac{1}{2} g_2^1(z, 0, \mu) + \frac{1}{3!} g_3^1(z, 0, \mu) + o(\mu|z|^2),$$

where g_2^1 and g_3^1 are the second and third terms in (z, μ) , respectively, given by

$$g_2^1(z, 0, \alpha) = \text{Proj}_{\text{Ker}(M_2^1)} f_2^1(z, 0, \mu), \quad g_3^1(z, 0, 0) = \text{Proj}_{\text{Ker}(M_3^1)} \tilde{f}_3^1(z, 0, \mu). \tag{3.13}$$

Here, $\frac{1}{3!} \tilde{f}_3^1$ is the term of order 3 obtained after the changes of variables in the previous step given by

$$\begin{aligned} \tilde{f}_3^1(z, 0, \mu) = & f_3^1(z, 0, \mu) + \frac{3}{2} [(D_z f_2^1)(z, 0, \mu) U_2^1(z, \mu) \\ & + (D_w f_2^1)(z, 0, \mu) U_2^2(z, \mu) - (D_z U_2^1(z, \mu)) g_2^1(z, 0, \mu)], \end{aligned} \tag{3.14}$$

and the operators M_j^1 and M_j^2 are defined by

$$\begin{aligned} M_j^1 : V_j^5(\mathbb{C}^2) &\rightarrow V_j^5(\mathbb{C}^2), M_j^1(U_j^1) = (D_z U_j^1(z, \mu) B_k z) - B_k U_j^1(z, \mu), \\ M_j^2 : V_j^5(X^s) &\rightarrow V_j^5(X^s), M_j^2(U_j^2) = (D_z U_j^2(z, \mu) B_k z) - \mathcal{L}(U_j^2(z, \mu)), \end{aligned} \tag{3.15}$$

where $V_j^5(Y)$ denotes the space of homogeneous polynomials of degree j in 5 variables $z_1, z_2, z_3, \mu_1, \mu_2$ with coefficients in Y . By (3.15) and noticing that B is a diagonal matrix, it is easy to verify from (3.15) that

$$\begin{aligned} M_j^1(z^m \mu^\ell e_r) &= D_z(z^m \mu^\ell e_r) B z - B z^m \mu^\ell e_r = i\omega_c (m_1 - m_2 + (-1)^r) z^m \mu^\ell e_r, \\ M_j^1(z^m \mu^\ell e_3) &= D_z(z^m \mu^\ell e_3) B z - B z^m \mu^\ell e_3 = i\omega_c (m_1 - m_2) z^m \mu^\ell e_3, \end{aligned} \tag{3.16}$$

where $r = 1, 2$ and $\{e_1, e_2, e_3\}$ is the canonical basis of \mathbb{R}^3 , $m = (m_1, m_2, m_3) \in \mathbb{N}_0^3, \ell = (\ell_1, \ell_2) \in \mathbb{N}_0^2, m_1 + m_2 + m_3 + \ell_1 + \ell_2 = j$. Therefore,

$$\text{Ker}(M_2^1) = \text{span} \left\{ \begin{pmatrix} z_1 z_3 \\ 0 \\ 0 \end{pmatrix}, \begin{pmatrix} z_1 \mu_i \\ 0 \\ 0 \end{pmatrix}, \begin{pmatrix} 0 \\ z_2 z_3 \\ 0 \end{pmatrix}, \begin{pmatrix} 0 \\ z_2 \mu_i \\ 0 \end{pmatrix}, \begin{pmatrix} 0 \\ 0 \\ z_1 z_2 \end{pmatrix}, \begin{pmatrix} 0 \\ 0 \\ z_3^2 \end{pmatrix}, \begin{pmatrix} 0 \\ 0 \\ z_3 \mu_i \end{pmatrix}, \begin{pmatrix} 0 \\ 0 \\ \mu_1 \mu_2 \end{pmatrix}, \begin{pmatrix} 0 \\ 0 \\ \mu_i^2 \end{pmatrix} \right\} \tag{3.17}$$

and

$$\begin{aligned} \text{Ker}(M_3^1) = \text{span} \left\{ \begin{pmatrix} z_1^2 z_2 \\ 0 \\ 0 \end{pmatrix}, \begin{pmatrix} z_1 z_3^2 \\ 0 \\ 0 \end{pmatrix}, \begin{pmatrix} z_1 z_3 \mu_i \\ 0 \\ 0 \end{pmatrix}, \begin{pmatrix} z_1 \mu_i^2 \\ 0 \\ 0 \end{pmatrix}, \begin{pmatrix} 0 \\ z_1 z_2^2 \\ 0 \end{pmatrix}, \begin{pmatrix} 0 \\ z_2 z_3^2 \\ 0 \end{pmatrix}, \begin{pmatrix} 0 \\ z_2 z_3 \mu_i \\ 0 \end{pmatrix}, \begin{pmatrix} 0 \\ z_2 \mu_i^2 \\ 0 \end{pmatrix}, \right. \\ \left. \begin{pmatrix} 0 \\ 0 \\ z_1 z_2 z_3 \end{pmatrix}, \begin{pmatrix} 0 \\ 0 \\ z_3^3 \end{pmatrix}, \begin{pmatrix} 0 \\ 0 \\ z_1 z_2 \mu_i \end{pmatrix}, \begin{pmatrix} 0 \\ 0 \\ z_3 \mu_i^2 \end{pmatrix} \right\}, \quad i = 1, 2. \end{aligned} \tag{3.18}$$

In order to simply the notation, we introduce the operator $\mathcal{H} : V_j^5(\mathbb{C}) \rightarrow V_j^5(\mathbb{C}^2)$ such that $\mathcal{H}(\xi_1 + \xi_2) = \mathcal{H}(\xi_1) + \mathcal{H}(\xi_2), \xi_1, \xi_2 \in V_j^5(\mathbb{C})$, and

$$\mathcal{H} \left(\alpha z_1^{m_1} z_2^{m_2} z_3^{m_3} \mu_1^{\ell_1} \mu_2^{\ell_2} \right) = \begin{pmatrix} \alpha z_1^{m_1} z_2^{m_2} z_3^{m_3} \mu_1^{\ell_1} \mu_2^{\ell_2} \\ \bar{\alpha} z_1^{m_2} z_2^{m_1} z_3^{m_3} \mu_1^{\ell_1} \mu_2^{\ell_2} \end{pmatrix}, \quad \alpha \in \mathbb{C}.$$

3.1. Calculation of $g_2^1(z, 0, \mu)$

By (3.2) and a direct computation, we have $f_{0020} = f_{0110} = f_{0002} = (0, 0)^T$. So,

$$\frac{1}{2} f_2(U, \mu) = (f_{1010} \bar{u} + f_{0110} v) \mu_1 + (f_{1001} u + f_{0101} v) \mu_2 + \frac{1}{2} f_{2000} u^2 + f_{1100} uv + \frac{1}{2} f_{0200} v^2, \tag{3.19}$$

which, together with (3.7), leads to

$$\begin{aligned} \frac{1}{2} f_2(z, 0, \mu) &= \frac{1}{2} f_2((z_1 p_0 + z_2 \bar{p}_0) \gamma_0(x) + z_3 p_n \gamma_n(x), \mu) \\ &= \mu_1 (((z_1 p_{01} + z_2 \bar{p}_{01}) \gamma_0(x) + z_3 p_{n1} \gamma_n(x)) f_{1010} + ((z_1 p_{02} + z_2 \bar{p}_{02}) \gamma_0(x) + z_3 p_{n2} \gamma_n(x)) f_{0110}) \\ &\quad + \mu_2 (((z_1 p_{01} + z_2 \bar{p}_{01}) \gamma_0(x) + z_3 p_{n1} \gamma_n(x)) f_{1001} + ((z_1 p_{02} + z_2 \bar{p}_{02}) \gamma_0(x) + z_3 p_{n2} \gamma_n(x)) f_{0101}) \\ &\quad + F_{110} \gamma_0^2(x) z_1 z_2 + F_{101} \gamma_0(x) \gamma_n(x) z_1 z_3 + F_{011} \gamma_0(x) \gamma_n(x) z_2 z_3, \\ &\quad + \frac{1}{2} (F_{200} \gamma_0^2(x) z_1^2 + F_{020} \gamma_0^2(x) z_2^2 + F_{002} \gamma_n^2(x) z_3^2), \end{aligned} \tag{3.20}$$

where

$$\begin{aligned} F_{200} &= p_{01}^2 f_{2000} + 2p_{01} p_{02} f_{1100} + p_{02}^2 f_{0200} = \bar{F}_{020}, \\ F_{002} &= p_{n1}^2 f_{2000} + 2p_{n1} p_{n2} f_{1100} + p_{n2}^2 f_{0200}, \\ F_{110} &= |p_{01}|^2 f_{2000} + 2\text{Re}\{p_{01} \bar{p}_{02}\} f_{1100} + |p_{02}|^2 f_{0200}, \\ F_{101} &= p_{01} p_{n1} f_{2000} + (p_{01} p_{n2} + p_{02} p_{n1}) f_{1100} + p_{02} p_{n2} f_{0200} = \bar{F}_{011}. \end{aligned}$$

Thus, from (3.12), (3.13), (3.17) and (3.20), we obtain

$$\begin{aligned} \frac{1}{2}g_2^1(z, 0, \mu) &= \frac{1}{2}\text{Proj}_{\text{Ker}(M_2^1)}f_2^1(z, 0, \mu) \\ &= \begin{pmatrix} \mathcal{H}((B_{11}\mu_1 + B_{21}\mu_2)z_1 + B_{101}z_1z_3) \\ (B_{13}\mu_1 + B_{23}\mu_2)z_3 + B_{110}z_1z_2 + B_{002}z_3^2 \end{pmatrix}, \end{aligned} \tag{3.21}$$

where

$$\begin{aligned} B_{11} &= p_{01}(q_0^T f_{1010}) + p_{02}(q_0^T f_{0110}), & B_{21} &= p_{01}(q_0^T f_{1001}) + p_{02}(q_0^T f_{0101}), \\ B_{13} &= p_{n1}(q_n^T f_{1010}) + p_{n2}(q_n^T f_{0110}), & B_{23} &= p_{n1}(q_n^T f_{1001}) + p_{n2}(q_n^T f_{0101}), \\ B_{101} &= q_0^T F_{101} \int_0^\pi \gamma_0^2(x)\gamma_n(x)dx = 0, & B_{110} &= q_n^T F_{110} \int_0^\pi \gamma_0^2(x)\gamma_n(x)dx = 0, \\ B_{002} &= q_n^T F_{002} \int_0^\pi \gamma_n^3(x)dx = 0. \end{aligned}$$

3.2. Calculation of $g_3^1(z, 0, \mu)$

Since $g_2^1(z, 0, 0) = 0$, it follows from (3.14) that the third term $g_3^1(z, 0, 0)$ can be determined as follows. By (3.12), (3.13) and (3.18), we have

$$\begin{aligned} g_3^1(z, 0, \mu) &= \text{Proj}_{\text{Ker}(M_3^1)}\tilde{f}_3^1(z, 0, \mu) \\ &= \text{Proj}_{S_1}\tilde{f}_3^1(z, 0, 0) + O(|z||\mu|^2 + |z|^2|\mu|), \end{aligned} \tag{3.22}$$

where

$$S_1 = \text{span} \left\{ \begin{pmatrix} z_1^2 z_2 \\ 0 \\ 0 \end{pmatrix}, \begin{pmatrix} z_1 z_2^2 \\ 0 \\ 0 \end{pmatrix}, \begin{pmatrix} 0 \\ z_1 z_2^2 \\ 0 \end{pmatrix}, \begin{pmatrix} 0 \\ z_2 z_3^2 \\ 0 \end{pmatrix}, \begin{pmatrix} 0 \\ 0 \\ z_1 z_2 z_3 \end{pmatrix}, \begin{pmatrix} 0 \\ 0 \\ z_3^3 \end{pmatrix} \right\}.$$

Here, $\tilde{f}_3^1(z, 0, 0)$ is determined by (3.14) with

$$U_2^1(z, 0) = (M_2^1)^{-1}\text{Proj}_{\text{Im}(M_2^1)}f_2^1(z, 0, 0) \tag{3.23}$$

and

$$(M_2^2 U_2^2)(z, 0) = f_2^2(z, 0, 0).$$

Next we compute the third order term $g_3^1(z, 0, 0) = \text{Proj}_{S_1}\tilde{f}_3^1(z, 0, 0)$ step by step in terms of (3.13) and (3.14).

Step 1. The calculation of $\text{Proj}_{S_1}f_3^1(x, 0, 0)$. Notice that

$$\int_0^\pi \gamma_0^4(x)dx = \int_0^\pi \gamma_0^2(x)\gamma_n^2(x)dx = \frac{1}{\pi}, \quad \int_0^\pi \gamma_n^4(x)dx = \frac{3}{2\pi}.$$

It follows from (3.2) and (3.12) that

$$\frac{1}{3!}\text{Proj}_{S_1}f_3^1(z, 0, 0) = \begin{pmatrix} \mathcal{H}(C_{210}z_1^2z_2 + C_{102}z_1z_3^2) \\ C_{111}z_1z_2z_3 + C_{003}z_3^3 \end{pmatrix}, \tag{3.24}$$

where

$$\begin{aligned} C_{210} &= \frac{1}{\pi}q_0^T F_{210}, & C_{102} &= \frac{1}{\pi}q_0^T F_{102}, \\ C_{111} &= \frac{1}{\pi}q_n^T F_{111}, & C_{003} &= \frac{3}{2\pi}q_n^T F_{003}, \end{aligned}$$

with

$$\begin{aligned} F_{210} &= \frac{1}{2}(f_{3000}|p_{01}|^2 p_{01} + f_{0300}|p_{02}|^2 p_{02} + f_{2100}(p_{01}^2 \bar{p}_{02} + 2|p_{01}|^2 p_{02}) + f_{1200}(p_{02}^2 \bar{p}_{01} + 2|p_{02}|^2 p_{01})), \\ F_{102} &= \frac{1}{2}(f_{3000}p_{01}p_{n1}^2 + f_{0300}p_{02}p_{n2}^2 + f_{2100}(p_{02}p_{n1}^2 + 2p_{01}p_{n1}p_{n2}) + f_{1200}(p_{01}p_{n2}^2 + 2p_{02}p_{n1}p_{n2})), \end{aligned}$$

$$F_{111} = (f_{3000} |p_{01}|^2 p_{n1} + f_{0300} |p_{02}|^2 p_{n2} + f_{2100} (|p_{01}|^2 p_{n2} + 2p_{n1} \operatorname{Re} \{p_{01} \bar{p}_{02}\}) + f_{1200} (|p_{02}|^2 p_{n1} + 2p_{n2} \operatorname{Re} \{p_{02} \bar{p}_{01}\})),$$

$$F_{003} = \frac{1}{3!} (f_{3000} p_{n1}^3 + f_{0300} p_{n2}^3) + \frac{1}{2} (f_{2100} p_{n1}^2 p_{n2} + f_{1200} p_{n1} p_{n2}^2).$$

Step 2. The calculation of $\operatorname{Proj}_S [(D_x f_2^1)(z, 0, 0)U_2^1(z, 0)]$. It follows from (3.12) and (3.20) that

$$f_2^1(z, 0, 0) = \frac{1}{\sqrt{\pi}} \Psi \begin{pmatrix} F_{200}z_1^2 + F_{020}z_2^2 + F_{002}z_3^2 + 2F_{110}z_1z_2 \\ 2F_{101}z_1z_3 + 2F_{011}z_2z_3 \end{pmatrix}, \tag{3.25}$$

where we have used the fact that

$$c_{kj} = \int_0^\pi \gamma_k^2(x) \gamma_j(x) dx = \begin{cases} \frac{1}{\sqrt{\pi}}, & j = k = 0, \\ \frac{1}{\sqrt{\pi}}, & j = 0, k \neq 0, \\ \frac{1}{\sqrt{2\pi}}, & j = 2k \neq 0, \\ 0, & \text{otherwise.} \end{cases}$$

By (3.23) and (3.25), we obtain

$$U_2^1(z, 0) = (M_2^1)^{-1} \operatorname{Proj}_{\operatorname{Im}(M_2^1)} f_2^1(z, 0, 0)$$

$$= \frac{1}{i\omega_c \sqrt{\pi}} \begin{pmatrix} q_0^T \left(F_{200}z_1^2 - \frac{1}{3}F_{020}z_2^2 - F_{002}z_3^2 - 2F_{110}z_1z_2 \right) \\ \bar{q}_0^T \left(\frac{1}{3}F_{200}z_1^2 - F_{020}z_2^2 + F_{002}z_3^2 + 2F_{110}z_1z_2 \right) \\ q_n^T (2F_{101}z_1z_3 - 2F_{011}z_2z_3) \end{pmatrix}.$$

So,

$$\frac{1}{3!} \operatorname{Proj}_{S_1} (D_z f_2^1(z, 0, 0)U_2^1(z, 0)) = \begin{pmatrix} \mathcal{H} (D_{210}z_1^2z_2 + D_{102}z_1z_3^2) \\ D_{111}z_1z_2z_3 + D_{003}z_3^3 \end{pmatrix}, \tag{3.26}$$

where

$$D_{210} = \frac{1}{3\pi \omega_c i} \left(- (q_0^T F_{200}) (q_0^T F_{110}) + \frac{1}{3} |q_0^T F_{020}|^2 + 2 |q_0^T F_{110}|^2 \right),$$

$$D_{102} = \frac{1}{3\pi \omega_c i} \left(- (q_0^T F_{200}) (q_0^T F_{002}) + (q_0^T F_{110}) (\bar{q}_0^T F_{002}) + 2 (q_0^T F_{002}) (q_n^T F_{101}) \right),$$

$$D_{111} = -\frac{4}{3\pi \omega_c} \operatorname{Im} \{ (q_0^T F_{110}) (q_n^T F_{101}) \},$$

$$D_{003} = -\frac{2}{3\pi \omega_c} \operatorname{Im} \{ (q_0^T F_{002}) (q_n^T F_{101}) \}.$$

Step 3. The calculation of $\operatorname{Proj}_S [(D_w f_2^1)(z, 0, 0)U_2^2(z, 0)]$.

Let

$$U_2^2(z, 0) : h(z) = \sum_{j \geq 0} (h_j(z))^T \begin{pmatrix} \beta_j^1 \\ \beta_j^2 \end{pmatrix},$$

with

$$h_j(z) = \begin{pmatrix} h_j^{(1)}(z) \\ h_j^{(2)}(z) \end{pmatrix} = \sum_{m_1+m_2+m_3=2j} \begin{pmatrix} h_{j m_1 m_2 m_3}^{(1)} \\ h_{j m_1 m_2 m_3}^{(2)} \end{pmatrix} z_1^{m_1} z_2^{m_2} z_3^{m_3}.$$

From (3.9) and (3.12), we get

$$\begin{aligned}
 (D_w f_2^1)(z, 0, 0)(h) &= \Psi \left(\left[D_w f_2 \left((\Phi_0 \quad \Phi_n) \begin{pmatrix} z_1 \gamma_0(x) \\ z_2 \gamma_0(x) \\ z_3 \gamma_n(x) \end{pmatrix}, 0 \right) (h), \beta_\zeta^1 \right] \right)_{\zeta=0}^n \\
 &= \Psi \left(\left[D_w f_2 \left((\Phi_0 \quad \Phi_n) \begin{pmatrix} z_1 \gamma_0(x) \\ z_2 \gamma_0(x) \\ z_3 \gamma_n(x) \end{pmatrix}, 0 \right) \left(\sum_{j=0,n} h_j^T \begin{pmatrix} \beta_j^1 \\ \beta_j^2 \end{pmatrix} \right), \beta_\zeta^1 \right] \right)_{\zeta=0}^n \\
 &\quad + \Psi \left(\left[D_w f_2 \left((\Phi_0 \quad \Phi_n) \begin{pmatrix} z_1 \gamma_0(x) \\ z_2 \gamma_0(x) \\ z_3 \gamma_n(x) \end{pmatrix}, 0 \right) \left(\sum_{j \neq 0,n} h_j^T \begin{pmatrix} \beta_j^1 \\ \beta_j^2 \end{pmatrix} \right), \beta_\zeta^2 \right] \right)_{\zeta=0}^n .
 \end{aligned}$$

By (3.19) and a direct computation, we obtain

$$\begin{aligned}
 &\left(\left[D_w f_2 \left((\Phi_0 \quad \Phi_n) \begin{pmatrix} z_1 \gamma_0(x) \\ z_2 \gamma_0(x) \\ z_3 \gamma_n(x) \end{pmatrix}, 0 \right) \left(h_j^T \begin{pmatrix} \beta_j^1 \\ \beta_j^2 \end{pmatrix} \right), \beta_\zeta^1 \right] \right) \\
 &\left(\left[D_w f_2 \left((\Phi_0 \quad \Phi_n) \begin{pmatrix} z_1 \gamma_0(x) \\ z_2 \gamma_0(x) \\ z_3 \gamma_n(x) \end{pmatrix}, 0 \right) \left(h_j^T \begin{pmatrix} \beta_j^1 \\ \beta_j^2 \end{pmatrix} \right), \beta_\zeta^2 \right] \right) \\
 &= 2 \{ f_{2000} (c_{0j\zeta} (z_1 p_{01} + z_2 \bar{p}_{01}) + c_{nj\zeta} z_3 p_{n1}) + f_{1100} (c_{0j\zeta} (z_1 p_{02} + z_2 \bar{p}_{02}) + c_{nj\zeta} z_3 p_{n2}) \} h_j^{(1)} \\
 &\quad + 2 \{ f_{0200} (c_{0j\zeta} (z_1 p_{02} + z_2 \bar{p}_{02}) + c_{nj\zeta} z_3 p_{n2}) + f_{1100} (c_{0j\zeta} (z_1 p_{01} + z_2 \bar{p}_{01}) + c_{nj\zeta} z_3 p_{n1}) \} h_j^{(2)},
 \end{aligned}$$

where

$$c_{0j0} = \begin{cases} \frac{1}{\sqrt{\pi}}, & j = 0, \\ 0, & j \neq 0, \end{cases} \quad c_{0jn} = c_{nj0} = \begin{cases} \frac{1}{\sqrt{\pi}}, & j = n, \\ 0, & j \neq n, \end{cases}$$

and

$$c_{njn} = \begin{cases} \frac{1}{\sqrt{\pi}}, & j = 0, \\ \frac{1}{\sqrt{2\pi}}, & j = 2n, \\ 0, & \text{otherwise.} \end{cases}$$

So,

$$(D_w f_2^1)(z, 0, 0)(h) = \Psi (G_{0\zeta} + G_{n\zeta})_{\zeta=0}^n,$$

where

$$\begin{aligned}
 G_{00} &= \frac{2}{\sqrt{\pi}} ((z_1 p_{01} + z_2 \bar{p}_{01}) f_{2000} + (z_1 p_{02} + z_2 \bar{p}_{02}) f_{1100}) h_0^{(1)} \\
 &\quad + \frac{2}{\sqrt{\pi}} ((z_1 p_{02} + z_2 \bar{p}_{02}) f_{0200} + (z_1 p_{01} + z_2 \bar{p}_{01}) f_{1100}) h_0^{(2)}, \\
 G_{n0} &= \frac{2}{\sqrt{\pi}} (z_3 p_{n1} f_{2000} + z_3 p_{n2} f_{1100}) h_n^{(1)} + \frac{2}{\sqrt{\pi}} (z_3 p_{n2} f_{0200} + z_3 p_{n1} f_{1100}) h_n^{(2)},
 \end{aligned}$$

$$G_{0n} = \frac{2}{\sqrt{\pi}} \{ (z_1 p_{01} + z_2 \bar{p}_{01}) f_{2000} + (z_1 p_{02} + z_2 \bar{p}_{02}) f_{1100} \} h_n^{(1)} + \frac{2}{\sqrt{\pi}} \{ (z_1 p_{02} + z_2 \bar{p}_{02}) f_{0200} + (z_1 p_{01} + z_2 \bar{p}_{01}) f_{1100} \} h_n^{(2)},$$

$$G_{nn} = (z_3 p_{n1} f_{2000} + z_3 p_{n2} f_{1100}) \left(\frac{2}{\sqrt{\pi}} h_0^{(1)} + \frac{2}{\sqrt{2\pi}} h_{2n}^{(1)} \right) + (z_3 p_{n2} f_{0200} + z_3 p_{n1} f_{1100}) \left(\frac{2}{\sqrt{\pi}} h_0^{(2)} + \frac{2}{\sqrt{2\pi}} h_{2n}^{(2)} \right).$$

So,

$$\frac{1}{3!} \text{Proj}_{S_1} (D_w f_2^1(z, 0, 0) U_2^2(z, 0)) = \begin{pmatrix} \mathcal{H} (E_{210} z_1^2 z_2 + E_{102} z_1 z_3^2) \\ E_{111} z_1 z_2 z_3 + E_{003} z_3^3 \end{pmatrix}, \tag{3.27}$$

where

$$E_{210} = \frac{1}{3\sqrt{\pi}} q_0^T \left((p_{01} f_{2000} + p_{02} f_{1100}) h_{0110}^{(1)} + (p_{02} f_{0200} + p_{01} f_{1100}) h_{0110}^{(2)} + (\bar{p}_{01} f_{2000} + \bar{p}_{02} f_{1100}) h_{0200}^{(1)} + (\bar{p}_{02} f_{0200} + \bar{p}_{01} f_{1100}) h_{0200}^{(2)} \right),$$

$$E_{102} = \frac{1}{3\sqrt{\pi}} q_0^T \left((p_{01} f_{2000} + p_{02} f_{1100}) h_{0002}^{(1)} + (p_{02} f_{0200} + p_{01} f_{1100}) h_{0002}^{(2)} + (p_{n1} f_{2000} + p_{n2} f_{1100}) h_{n101}^{(1)} + (p_{n2} f_{0200} + p_{n1} f_{1100}) h_{n101}^{(2)} \right),$$

$$E_{111} = \frac{1}{3\sqrt{\pi}} q_n^T \left((p_{01} f_{2000} + p_{02} f_{1100}) h_{n011}^{(1)} + (p_{02} f_{0200} + p_{01} f_{1100}) h_{n011}^{(2)} + (\bar{p}_{01} f_{2000} + \bar{p}_{02} f_{1100}) h_{n101}^{(1)} + (\bar{p}_{02} f_{0200} + \bar{p}_{01} f_{1100}) h_{n101}^{(2)} \right) + q_n^T \left((p_{n1} f_{2000} + p_{n2} f_{1100}) \left(\frac{1}{3\sqrt{\pi}} h_{0110}^{(1)} + \frac{1}{3\sqrt{2\pi}} h_{(2n)110}^{(1)} \right) + (p_{n2} f_{0200} + p_{n1} f_{1100}) \left(\frac{1}{3\sqrt{\pi}} h_{0110}^{(2)} + \frac{1}{3\sqrt{2\pi}} h_{(2n)110}^{(2)} \right) \right),$$

$$E_{003} = q_n^T \left((p_{n1} f_{2000} + p_{n2} f_{1100}) \left(\frac{1}{3\sqrt{\pi}} h_{0002}^{(1)} + \frac{1}{3\sqrt{2\pi}} h_{(2n)002}^{(1)} \right) + (p_{n2} f_{0200} + p_{n1} f_{1100}) \left(\frac{1}{3\sqrt{\pi}} h_{0002}^{(2)} + \frac{1}{3\sqrt{2\pi}} h_{(2n)002}^{(2)} \right) \right).$$

Clearly, we still need to compute $h_j^{(1)}$ and $h_j^{(2)}$. By (3.10) and (3.20), we have

$$\begin{pmatrix} [H_2(z, 0, 0), \beta_0^1] \\ [H_2(z, 0, 0), \beta_0^2] \end{pmatrix} = \frac{1}{\sqrt{\pi}} (F_{200} - (q_0^T F_{200} p_0 + \bar{q}_0^T F_{200} \bar{p}_0)) z_1^2 + \frac{1}{\sqrt{\pi}} (F_{020} - (q_0^T F_{020} p_0 + \bar{q}_0^T F_{020} \bar{p}_0)) z_2^2 + \frac{1}{\sqrt{\pi}} (F_{002} - (q_0^T F_{002} p_0 + \bar{q}_0^T F_{002} \bar{p}_0)) z_3^2 + \frac{2}{\sqrt{\pi}} (F_{110} - (q_0^T F_{110} p_0 + \bar{q}_0^T F_{110} \bar{p}_0)) z_1 z_2,$$

$$\begin{pmatrix} [H_2(z, 0, 0), \beta_n^1] \\ [H_2(z, 0, 0), \beta_n^2] \end{pmatrix} = \frac{2}{\sqrt{\pi}} (F_{101} - q_n^T F_{101} p_n) z_1 z_3 + \frac{2}{\sqrt{\pi}} (F_{011} - q_n^T F_{011} p_n) z_2 z_3, \tag{3.28}$$

$$\begin{pmatrix} [H_2(z, 0, 0), \beta_{2n}^1] \\ [H_2(z, 0, 0), \beta_{2n}^2] \end{pmatrix} = \frac{1}{\sqrt{2\pi}} F_{002} z_3^2.$$

In addition, by (3.15), we have

$$M_2^2 \left((h_j(z))^T \begin{pmatrix} \beta_j^1 \\ \beta_j^2 \end{pmatrix} \right) = \left(D_z \left((h_j(z))^T \begin{pmatrix} \beta_j^1 \\ \beta_j^2 \end{pmatrix} \right) Bz \right) - \mathcal{L} \left((h_j(z))^T \begin{pmatrix} \beta_j^1 \\ \beta_j^2 \end{pmatrix} \right),$$

which leads to

$$\begin{pmatrix} \left[M_2^2 \left((h_j(z))^T \begin{pmatrix} \beta_j^1 \\ \beta_j^2 \end{pmatrix} \right), \beta_j^1 \right] \\ \left[M_2^2 \left((h_j(z))^T \begin{pmatrix} \beta_j^1 \\ \beta_j^2 \end{pmatrix} \right), \beta_j^2 \right] \end{pmatrix} = i\omega_c (2h_{j200}z_1^2 + h_{j101}z_1z_3 - 2h_{j020}z_2^2 - h_{j011}z_2z_3) + j^2 \begin{pmatrix} d_1 & 0 \\ 0 & d_2 \end{pmatrix} h_j(z) - L_0 h_j(z).$$

Notice that

$$\begin{pmatrix} \left[M_2^2 \left((h_j(z))^T \begin{pmatrix} \beta_j^1 \\ \beta_j^2 \end{pmatrix} \right), \beta_j^1 \right] \\ \left[M_2^2 \left((h_j(z))^T \begin{pmatrix} \beta_j^1 \\ \beta_j^2 \end{pmatrix} \right), \beta_j^2 \right] \end{pmatrix} = \begin{pmatrix} [H_2, \beta_j^1] \\ [H_2, \beta_j^2] \end{pmatrix}. \tag{3.29}$$

So, by (3.28) and (3.29) and matching the coefficients of $z_1^{m_1} z_2^{m_2} z_3^{m_3}$, we have

$$\begin{cases} j = 0, z_1^2 : & 2i\omega_c h_{0200} - L_0 (h_{0200}) = \frac{1}{\sqrt{\pi}} (F_{200} - (q_0^T F_{200} p_0 + \bar{q}_0^T F_{200} \bar{p}_0)), \\ j = 0, z_2^2 : & -2i\omega_c h_{0020} - L_0 (h_{0020}) = \frac{1}{\sqrt{\pi}} (F_{020} - (q_0^T F_{020} p_0 + \bar{q}_0^T F_{020} \bar{p}_0)), \\ j = 0, z_3^2 : & L_0 (h_{0002}) = -\frac{1}{\sqrt{\pi}} (F_{002} - (q_0^T F_{002} p_0 + \bar{q}_0^T F_{002} \bar{p}_0)), \\ j = 0, z_1 z_2 : & L_0 (h_{0110}) = -\frac{2}{\sqrt{\pi}} (F_{110} - (q_0^T F_{110} p_0 + \bar{q}_0^T F_{110} \bar{p}_0)), \\ j = n, z_1 z_3 : & i\omega_c h_{n101} + (\text{diag}(d_1 n^2, d_2 n^2) - L_0) h_{n101} = \frac{2}{\sqrt{\pi}} (F_{101} - q_n^T F_{101} p_n), \\ j = n, z_2 z_3 : & -i\omega_c h_{n011} + (\text{diag}(d_1 n^2, d_2 n^2) - L_0) h_{n011} = \frac{2}{\sqrt{\pi}} (F_{011} - q_n^T F_{011} p_n), \\ j = 2n, z_3^2 : & (\text{diag}(4d_1 n^2, 4d_2 n^2) - L_0) h_{(2n)002} = \frac{1}{\sqrt{2\pi}} F_{002}, \\ j = 2n, z_1 z_2 : & (\text{diag}(4d_1 n^2, 4d_2 n^2) - L_0) h_{(2n)110} = (0, 0)^T. \end{cases}$$

Solving these equations, we have

$$\begin{aligned} h_{0200} &= \frac{1}{\sqrt{\pi}} (2i\omega_c I - \mathcal{M}_0)^{-1} (F_{200} - (q_0^T F_{200} p_0 + \bar{q}_0^T F_{200} \bar{p}_0)), \\ h_{0020} &= \frac{1}{\sqrt{\pi}} (-2i\omega_c I - \mathcal{M}_0)^{-1} (F_{020} - (q_0^T F_{020} p_0 + \bar{q}_0^T F_{020} \bar{p}_0)), \\ h_{0002} &= -\frac{1}{\sqrt{\pi}} \mathcal{M}_0^{-1} (F_{002} - (q_0^T F_{002} p_0 + \bar{q}_0^T F_{002} \bar{p}_0)), \\ h_{0110} &= -\frac{2}{\sqrt{\pi}} \mathcal{M}_0^{-1} (F_{110} - (q_0^T F_{110} p_0 + \bar{q}_0^T F_{110} \bar{p}_0)), \\ h_{n101} &= \frac{2}{\sqrt{\pi}} (i\omega_c I - \mathcal{M}_n)^{-1} (F_{101} - q_n^T F_{101} p_n), \\ h_{n011} &= \frac{2}{\sqrt{\pi}} (-i\omega_c I - \mathcal{M}_n)^{-1} (F_{011} - q_n^T F_{011} p_n), \\ h_{(2n)002} &= -\frac{1}{\sqrt{2\pi}} \mathcal{M}_{2n}^{-1} F_{002}, \quad h_{(2n)110} = (0, 0)^T. \end{aligned}$$

Hence, by (3.30), (3.24), (3.26) and (3.27) we have

$$\frac{1}{3!}g_3^1(z, 0, 0) = \begin{pmatrix} \mathcal{H}[B_{210}z_1^2z_2 + B_{102}z_1z_3^2] \\ B_{111}z_1z_2z_3 + B_{003}z_3^3 \end{pmatrix}, \tag{3.30}$$

with

$$B_{210} = C_{210} + \frac{3}{2}(D_{210} + E_{210}), \quad B_{102} = C_{102} + \frac{3}{2}(D_{102} + E_{102}),$$

$$B_{111} = C_{111} + \frac{3}{2}(D_{111} + E_{111}), \quad B_{003} = C_{003} + \frac{3}{2}(D_{003} + E_{003}).$$

Therefore, by (3.21) and (3.30), the normal form for Hopf–Turing bifurcation reads as

$$\dot{z} = Bz + \begin{pmatrix} \mathcal{H}((B_{11}\mu_1 + B_{21}\mu_2)z_1) \\ (B_{13}\mu_1 + B_{23}\mu_2)z_3 \end{pmatrix} + \begin{pmatrix} \mathcal{H}(B_{210}z_1^2z_2 + B_{102}z_1z_3^2) \\ B_{111}z_1z_2z_3 + B_{003}z_3^3 \end{pmatrix} + O(|z||\mu|^2 + |z|^2|\mu| + |z|^4). \tag{3.31}$$

The normal form of Eq. (3.31) can now be written in real coordinates w through the change of variables $z_1 = v_1 - iv_2, z_2 = v_1 + iv_2, z_3 = v_3$, and then changing to cylindrical coordinates by $v_1 = \rho \cos \Theta, v_2 = \rho \sin \Theta, v_3 = r$, we obtain, truncating at third order terms and removing the azimuthal term,

$$\dot{\rho} = \alpha_1(\mu)\rho + \kappa_{11}\rho^3 + \kappa_{12}\rho r^2,$$

$$\dot{r} = \alpha_2(\mu)r + \kappa_{21}\rho^2r + \kappa_{22}r^3, \tag{3.32}$$

where

$$\alpha_1(\mu) = \text{Re}(B_{11})\mu_1 + \text{Re}(B_{21})\mu_2, \quad \alpha_2(\mu) = B_{13}\mu_1 + B_{23}\mu_2,$$

$$\kappa_{11} = \text{Re}(B_{210}), \quad \kappa_{12} = \text{Re}(B_{102}), \quad \kappa_{21} = B_{111}, \quad \kappa_{22} = B_{003}.$$

By the center manifold theorem due to Carr [53] and the bifurcation theorem [52,54], the dynamics of system (1.2) near the bifurcation value is topologically equivalent to that of the normal form near the sufficiently small neighborhood of $\mu = 0$. The dynamics of the normal form (3.32) in the sufficiently small neighborhood of the origin of the μ_1 – μ_2 plane is completely determined by the coefficients $\alpha_1(\mu), \alpha_2(\mu), \kappa_{ij}, i, j = 1, 2$. For all possible dynamics of the normal form (3.32), refer to the books [54,55].

4. Numerical simulations

In this section, we make some numerical simulations to support and extend our analytical results. Taking $d_1 = 0.02, d_2 = 0.2, c = 0.2$, the positive equilibrium E^* exists provided that $a > 0.8b$. It follows from (2.6), (2.8) and (2.10) that $n = 2$ and

$$H_0 : a = \frac{24}{25}b - \frac{4}{25}, \quad b > 1; \quad \ell_2 : a = \frac{14}{15}b - \frac{2}{25}, \quad \frac{27}{20} < b < \frac{147}{20}.$$

The straight line H_0 intersects with ℓ_2 at the point $P^*(3, 68/25)$ and system (1.2) undergoes Hopf–Turing bifurcation near the positive equilibrium $E^*(75/68, 1125/68)$ at the point P^* . According to the procedure in Section 3 with $n = 2$, the normal form truncated to the third order terms is

$$\dot{\rho} = (0.48\mu_1 - 0.5\mu_2)\rho - 0.0436\rho^3 - 0.3027\rho r^2,$$

$$\dot{r} = (1.0182\mu_1 - 1.0909\mu_2)r - 0.3296\rho^2r - 0.1953r^3. \tag{4.1}$$

Notice that $\rho > 0$ and r is an arbitrary real number. System (4.1) has a zero equilibrium $A_0 = (0, 0)$ for all μ_1, μ_2 , three trivial equilibria $A_1 = (\sqrt{0.48\mu_1 - 0.5\mu_2}, 0)$ for $0.48\mu_1 - 0.5\mu_2 > 0$ and $A_2^\pm = (0, \pm\sqrt{1.0182\mu_1 - 1.0909\mu_2})$ for $1.0182\mu_1 - 1.0909\mu_2 > 0$, and two nontrivial equilibria

$$A_3^\pm = (\sqrt{2.3502\mu_1 - 2.5485\mu_2}, \pm\sqrt{1.2472\mu_1 - 1.2847\mu_2})$$

for $2.3502\mu_1 - 2.5485\mu_2 > 0$ and $1.2472\mu_1 - 1.2847\mu_2 > 0$. Define the critical bifurcation lines as follows:

$$H : \mu_2 = \frac{24}{25}\mu_1; \quad T : \mu_2 = \frac{14}{15}\mu_1;$$

$$T_1 : \mu_2 = 0.9222\mu_1, \quad \mu_1 > 0; \quad T_2 : \mu_2 = 0.9708\mu_1, \quad \mu_1 < 0.$$

Then, according to the results in [54], the bifurcation diagram in the (μ_1, μ_2) parameter plane and the corresponding phase portraits of system (4.1) in the (ρ, r) plane can be shown in Fig. 1. The (μ_1, μ_2) parameter plane is divided into six regions characterized by the phase portraits (Fig. 1). Notice that the zero equilibrium A_0 of (4.1) corresponds to the

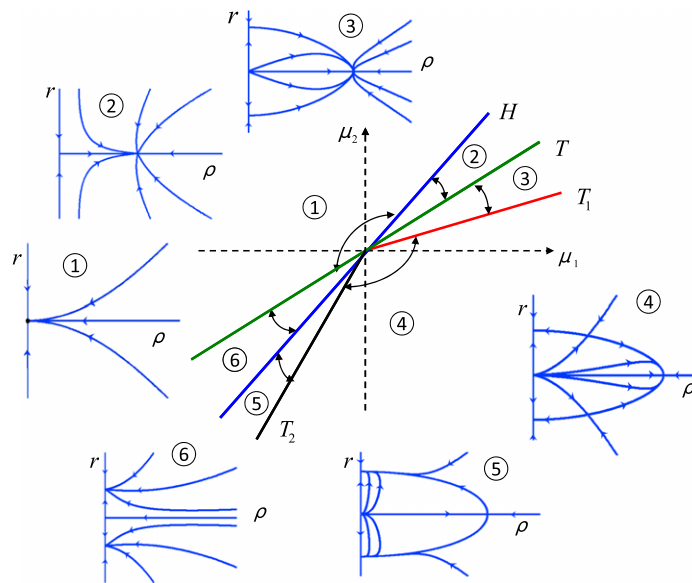


Fig. 1. Bifurcation and phase portraits of (4.1) near the point $P^* = (3, 68/25)$. Here, the origin of the μ_1 - μ_2 plane corresponds to the point $P^* = (3, 68/25)$ of the b - a plane.

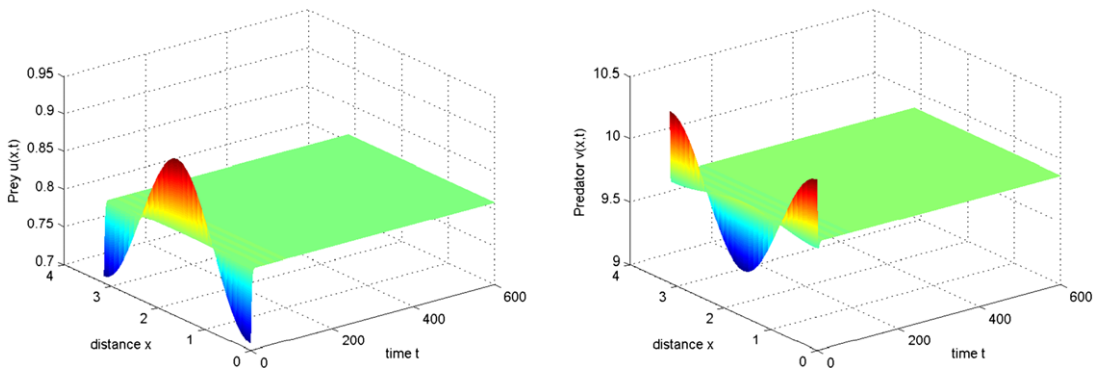


Fig. 2. When (μ_1, μ_2) lies in region ①, the positive constant equilibrium is asymptotically stable.

constant equilibrium E^* of the original system (1.2). The equilibrium A_1 in the ρ -axis of (4.1) corresponds to the spatially homogeneous periodic solution of the original system (1.2). The equilibria A_2^\pm in the r -axis of (4.1) correspond to the steady state solutions of the original system (1.2) like $\cos(2x)$ shape. While the nontrivial equilibria A_3^\pm generate solutions of the original system (1.2) with spatial structure like $\cos(2x)$ shape and periodic temporal structure.

Therefore, for system (1.2), the spatiotemporal dynamics near the Hopf–Turing bifurcation point P^* can be described by Fig. 1. In region ①, there is only one positive constant equilibrium which is asymptotically stable, as shown in Fig. 2. In region ②, the positive constant equilibrium becomes stable and only the Hopf bifurcation occurs. The emerging state of system (1.2) is homogeneously periodic oscillation. For $(\mu_1, \mu_2) = (0.05, 0.047) \in D_2$, Fig. 3 is the numerical simulation of the dynamics of system (1.2) with the initial values $u(x, 0) = 0.3604 - 0.0001 \cos(2x)$, $v(x, 0) = 4.3974 - 0.0002 \cos(2x)$, showing the existence of stable homogeneously periodic oscillation. In region ③, there are two spatially inhomogeneous steady states and a homogeneous periodic solution. The spatially inhomogeneous steady states are unstable and the homogeneous periodic solution is asymptotically stable, and there exists an orbit connecting the unstable steady state to the stable spatially homogeneous periodic solution. For $(\mu_1, \mu_2) = (0.05, 0.04612) \in D_3$ and the initial values $u(x, 0) = 0.3596 - 0.0001 \cos(2x)$, $v(x, 0) = 4.3870 - 0.0002 \cos(2x)$ close to the unstable spatially inhomogeneous steady state, Fig. 4 shows the existence of this connecting orbit.

In region ④, stable spatially inhomogeneous steady states and the homogeneous periodic solution coexist. The emerging state of system (1.2) is therefore either the homogeneous periodic solution or spatially inhomogeneous steady states depending on the selection of the initial values. For $(\mu_1, \mu_2) = (0.05, 0.04612) \in D_4$, Figs. 5–8 illustrate the dynamics of system (1.2) for different initial values. For these parameters, the positive constant equilibrium is $E^* = (0.3339, 4.0741)$. A small constant perturbation of this positive constant equilibrium yields a stable homogeneous periodic solution, as

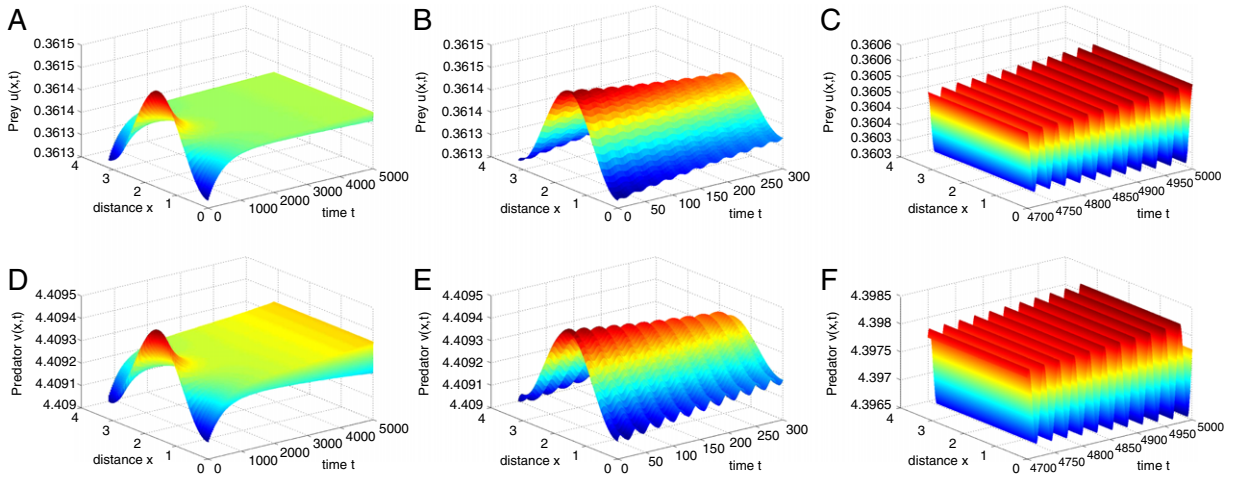


Fig. 3. When (μ_1, μ_2) lies in region ②, the positive constant equilibrium $E^*(0.3604, 4.3974)$ becomes unstable and there exists a stable spatially homogeneous periodic solution.

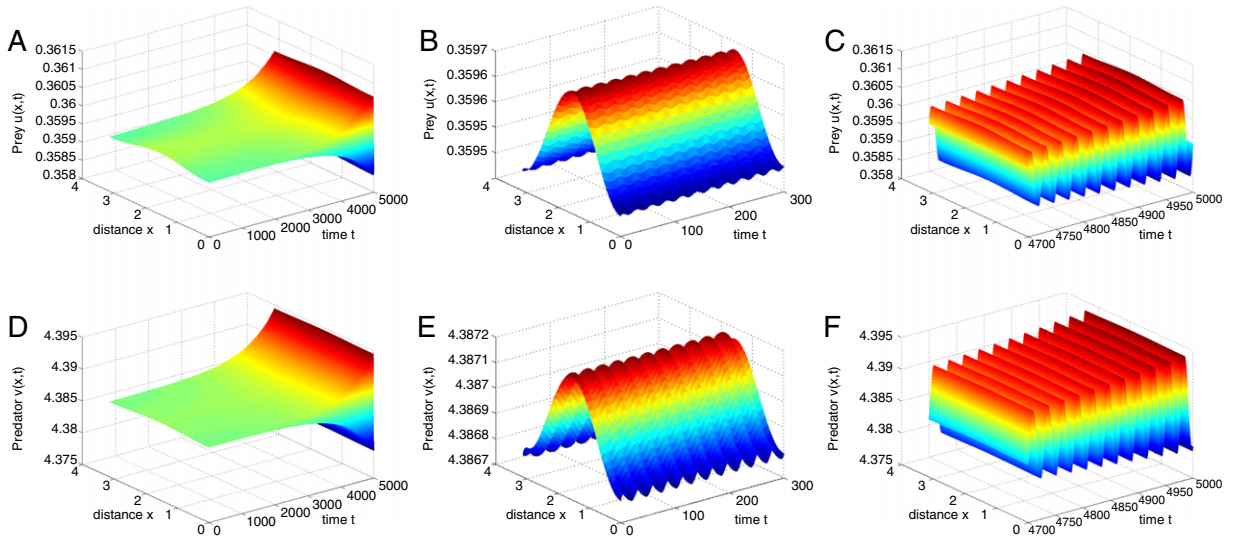


Fig. 4. When (μ_1, μ_2) lies in region ③, the positive constant equilibrium $E^*(0.3596, 4.3870)$ is unstable. There are unstable spatially inhomogeneous steady states and a stable homogeneous periodic solution and there exists an orbit connecting these two states.

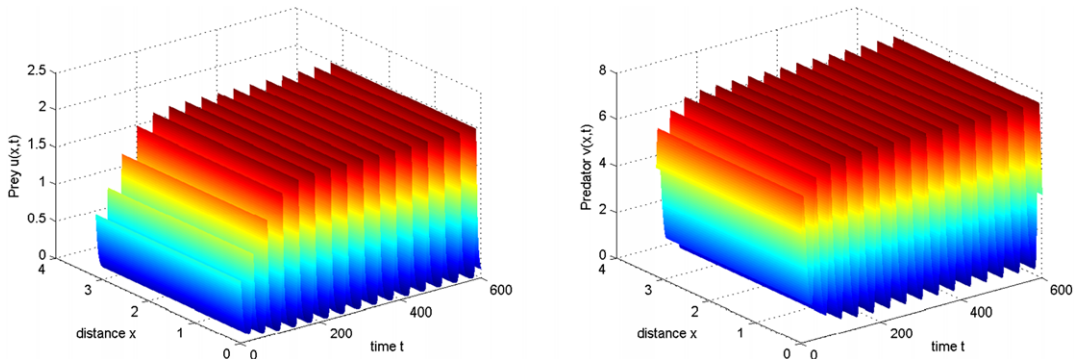


Fig. 5. Stable homogeneous periodic solution for (μ_1, μ_2) belonging to region ④, which coexists with two spatially inhomogeneous steady states as shown in Fig. 6.

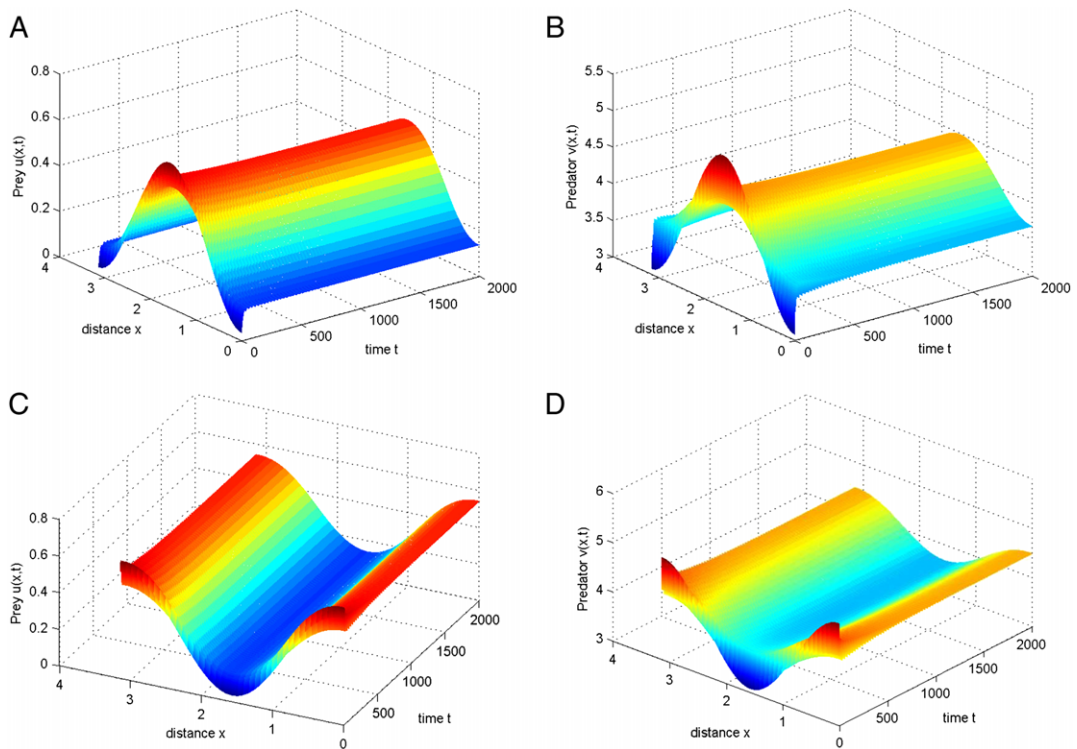


Fig. 6. Two spatially inhomogeneous steady states for (μ_1, μ_2) belonging to region ④, which coexist with the stable homogeneous periodic solution as shown in Fig. 5.

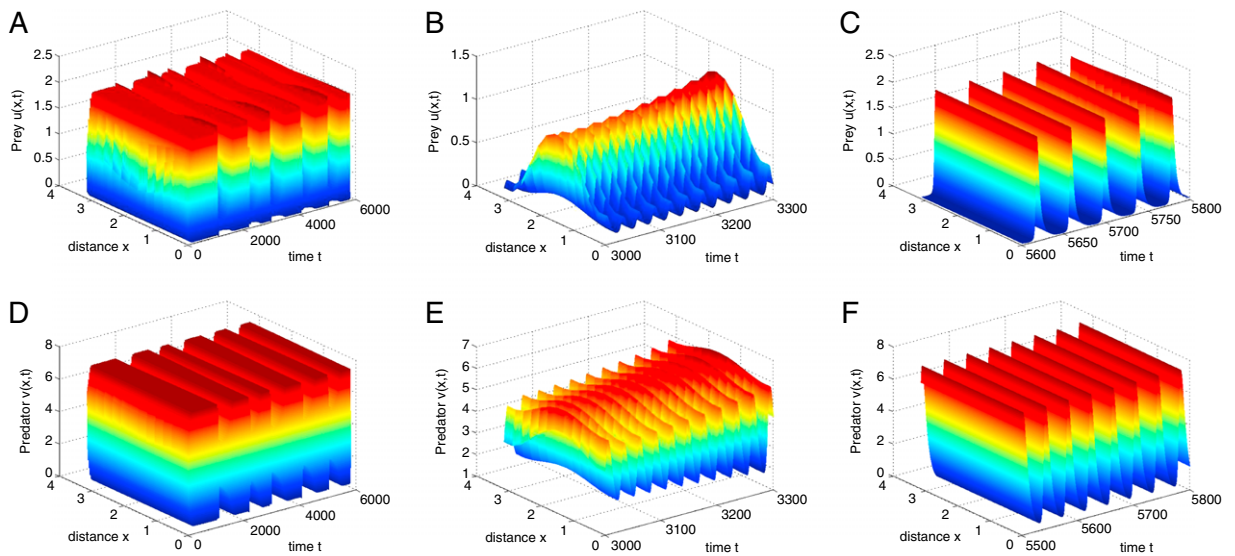


Fig. 7. The evolution of the spatiotemporal dynamics of system (1.2) for (μ_1, μ_2) belonging to region ④ and the initial values close to the unstable saddle. The system starts from a solution with certain spatiotemporal pattern and finally evolves into a stable homogeneous periodic solution.

shown in Fig. 5 with the initial values $u(x, 0) = 0.3339 + 0.5, v(x, 0) = 4.0741 + 0.6$. For the initial values close to spatially inhomogeneous steady states, the system finally evolves into spatially inhomogeneous steady state like $\cos(2x)$ shape. Fig. 6 illustrates the results for the initial values $u(x, 0) = 0.3339 - 0.5 \cos(2x), v(x, 0) = 4.0741 - 0.6 \cos(2x)$ and $u(x, 0) = 0.3339 + 0.5 \cos(2x), v(x, 0) = 4.0741 + 0.6 \cos(2x)$. In addition, notice that for (μ_1, μ_2) belonging to region ④ the normal form (4.1) has two unstable nontrivial equilibria A_3^\pm (saddle points). So, system (1.2) has unstable states with inhomogeneous spatial structure like $\cos(2x)$ shape and periodic temporal structure. Figs. 7 and 8 illustrate the

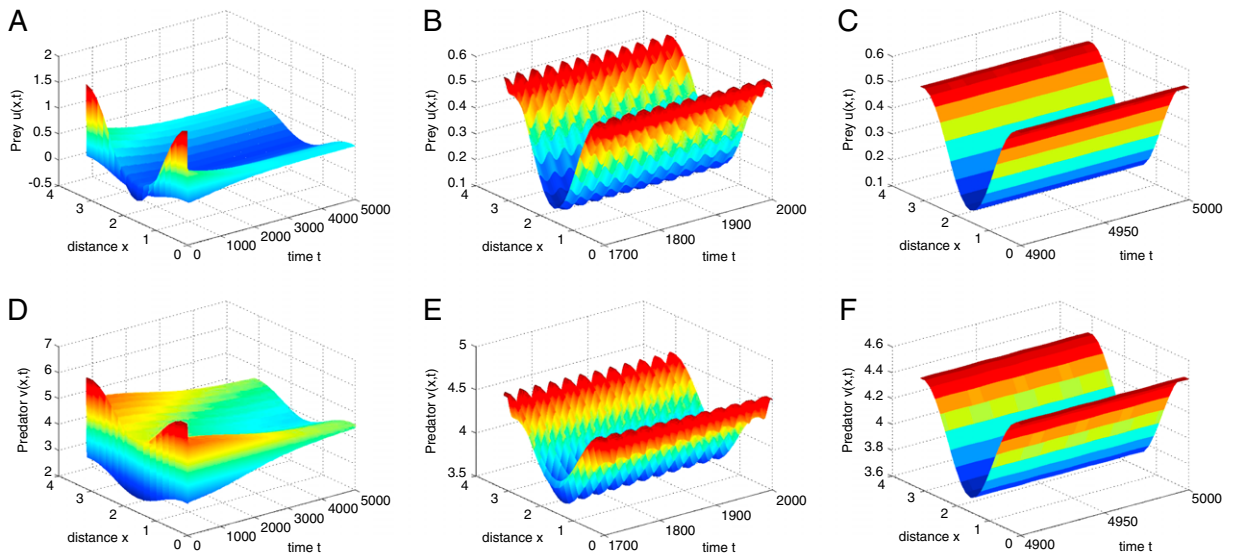


Fig. 8. The evolution of the spatiotemporal dynamics of system (1.2) for (μ_1, μ_2) belonging to region ④ and the initial values close to the unstable saddle. The system starts from a solution with certain spatiotemporal pattern and finally evolves into a stable spatially inhomogeneous steady state.

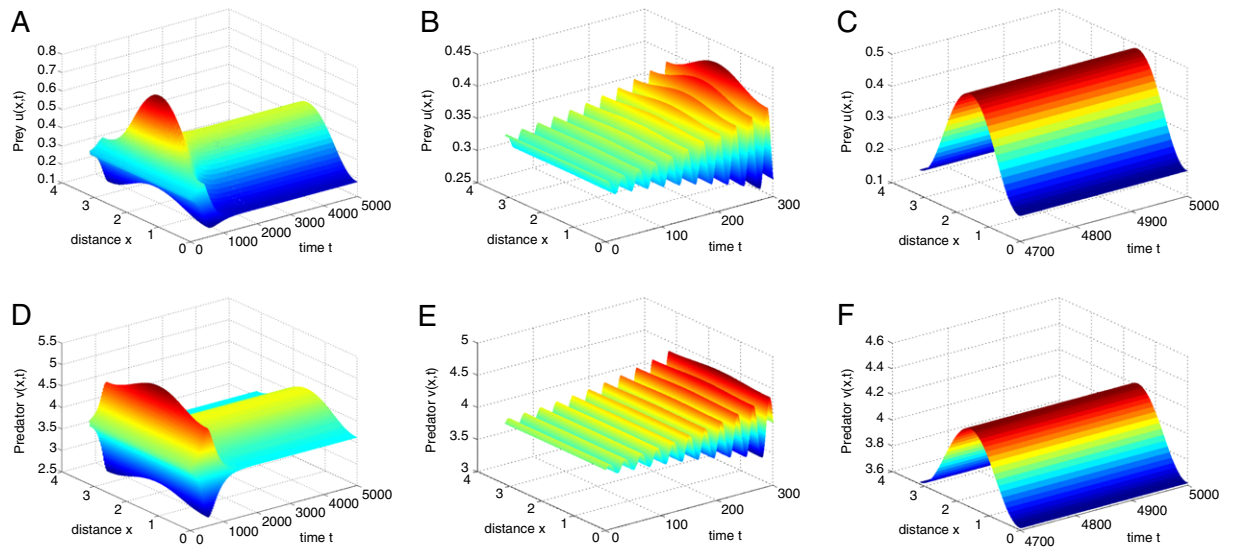


Fig. 9. When (μ_1, μ_2) lies in region ⑤, the positive constant equilibrium $E^*(0.3327, 3.9259)$ is unstable. There are stable spatially inhomogeneous steady states and an unstable homogeneous periodic solution and there exists an orbit connecting these two states.

spatiotemporal dynamics of system (1.2) for the initial values $u(x, 0) = 0.8 + 0.2 \cos(2x)$, $v(x, 0) = 4.8 + 0.3 \cos(2x)$, and $u(x, 0) = 0.3339 + 0.3 \cos(2x)$, $v(x, 0) = 4.0741 + \cos(2x)$, respectively.

In region ⑤, system (1.2) has two stable spatially inhomogeneous steady states (to that shown in Fig. 6) and an unstable homogeneous periodic solution. For the initial values $u(x, 0) = 0.3427 - 0.0003 \cos(2x)$, $v(x, 0) = 3.9359 - 0.001 \cos(2x)$ which is sufficiently small perturbation of the constant equilibrium $E^*(0.3327, 3.9259)$, Fig. 9 shows the existence of the orbit connecting the unstable homogeneous periodic solution to the stable spatially inhomogeneous steady state.

In region ⑥, system (1.2) has only two stable spatially inhomogeneous steady states. For any small perturbation of the positive constant equilibrium E^* , the system finally evolves into a stable spatially inhomogeneous steady state very similar to that shown in Fig. 6.

5. Conclusion

In this paper, we have studied the spatiotemporal dynamics of a ratio-dependent predator–prey model with diffusion near the Hopf–Turing bifurcation point. The normal form for the Hopf–Turing bifurcation has been derived. The classification

of the spatiotemporal patterns and their stability have been determined according to the corresponding normal form. The spatiotemporal dynamics near the Hopf–Turing bifurcation point can be explicitly classified into six scenarios: stable constant equilibrium; purely spatially pattern (spatially inhomogeneous steady state); purely temporarily periodic pattern (spatially homogeneous periodic solutions); coexistence of stable spatially pattern and unstable temporarily periodic pattern; coexistence of unstable spatially pattern and stable temporarily periodic pattern; bistability between spatial and temporal modes. In the region where the bistability occurs, there also exist the mixed spatiotemporal periodic patterns. These six bifurcation scenarios are well confirmed quantitatively by numerical simulations.

Acknowledgments

The first author is supported by the State Key Program of National Natural Science Foundation of China (No. 11032009), the Scientific Research Foundation for the Returned Overseas Chinese Scholars and the Program for New Century Excellent Talents in University (NCET-11-0385); and the second author is partially supported by Natural Science and Engineering Council of Canada (No. 227048-2010).

References

- [1] H.I. Freedman, *Deterministic Mathematical Models in Population Ecology*, Marcel Dekker, New York, 1980.
- [2] J.D. Murray, *Mathematical Biology II*, Springer-Verlag, Heidelberg, 2002.
- [3] C.S. Holling, The components of predation as revealed by a study of small-mammal predation of the European pine sawfly, *Can. Entomol.* 91 (1959) 293–320.
- [4] R. Arditi, L.R. Ginzburg, Coupling in predator–prey dynamics: ratio-dependence, *J. Theoret. Biol.* 139 (1989) 311–326.
- [5] R. Arditi, L.R. Ginzburg, H.R. Akçakaya, Variation in plankton densities among lakes: a case for ratio-dependent models, *Am. Nat.* 138 (1991) 1287–1296.
- [6] H.R. Akçakaya, R. Arditi, L.R. Ginzburg, Ratio-dependent predation: an abstraction that works, *Ecology* 76 (1995) 995–1004.
- [7] C.B. Huffaker, Experimental studies on predation: dispersion factors and predator–prey oscillations, *Hilgardia* 27 (1958) 343–383.
- [8] L.S. Luckinbill, Coexistence in laboratory populations of *Paramecium aurelia* and its predator *Dininium nasutum*, *Ecology* 53 (1973) 1320–1327.
- [9] N.G. Hairston, F.E. Smith, L.B. Slobodkin, Community structure, population control and competition, *Am. Nat.* 94 (1960) 421–425.
- [10] M.L. Rosenzweig, Paradox of enrichment: destabilization of exploitation systems in ecological time, *Science* 171 (1971) 385–387.
- [11] R.F. Luck, Evaluation of natural enemies for biological control: a behavioral evaluation, *Trends Ecol. Evol.* 5 (1990) 196–199.
- [12] A.A. Berryman, The origin and evolution of predator–prey theory, *Ecology* 73 (1992) 1530–1535.
- [13] C. Cosner, D.L. DeAngelis, J.S. Ault, D.B. Olson, Effects of spatial grouping on the functional response of predators, *Theor. Popul. Biol.* 56 (1999) 65–75.
- [14] O. Arino, A. El abdllaoui, J. Mikram, J. Chattopadhyay, Infection in prey population may act as a biological control in ratio-dependent predator–prey models, *Nonlinearity* 17 (2004) 1101–1116.
- [15] F. Berezovskaya, G. Karev, R. Arditi, Parametric analysis of the ratio-dependent predator–prey model, *J. Math. Biol.* 43 (2001) 221–246.
- [16] S.-B. Hsu, T.-W. Hwang, Y. Kuang, Global analysis of the Michaelis–Menten type ratio-dependent predator–prey system, *J. Math. Biol.* 42 (2001) 489–506.
- [17] S.-B. Hsu, T.-W. Hwang, Y. Kuang, Rich dynamics of a ratio-dependent one prey two predator model, *J. Math. Biol.* 43 (2001) 377–396.
- [18] C. Jost, O. Arino, R. Arditi, About deterministic extinction in ratio-dependent predator–prey models, *Bull. Math. Biol.* 61 (1999) 19–32.
- [19] Y. Kuang, E. Beretta, Global qualitative analysis of a ratio-dependent predator–prey system, *J. Math. Biol.* 36 (1998) 389–406.
- [20] Y. Kuang, Rich dynamics of Gause-type ratio-dependent predator–prey systems, *Fields Inst. Commun.* 21 (1999) 325–337.
- [21] S. Ruan, Y. Tang, W. Zhang, Versal unfoldings of predator–prey systems with ratio-dependent functional response, *J. Differential Equations* 249 (2010) 1410–1435.
- [22] D. Xiao, S. Ruan, Global dynamics of a ratio-dependent predator–prey systems, *J. Math. Biol.* 43 (2001) 221–290.
- [23] E. Beretta, Y. Kuang, Global analyses in some delayed ratio-dependent predator–prey systems, *Nonlinear Analysis, T.M.A.* 32 (1998) 381–408.
- [24] S. Tang, L. Chen, Global qualitative analysis for a ratio-dependent predator–prey model with delay, *J. Math. Anal. Appl.* 266 (2002) 401–419.
- [25] D. Xiao, W. Li, Stability and bifurcation in a delayed ratio-dependent predator–prey system, *Proc. Edinb. Math. Soc.* 45 (2003) 205–220.
- [26] R. Xu, F.A. Davidson, M.A.J. Chaplain, Persistence and stability for a two-species ratio-dependent predator–prey system with distributed time delay, *J. Math. Anal. Appl.* 269 (2002) 256–277.
- [27] D.G. Aronson, H.F. Weinberger, Nonlinear diffusion in population genetics, combustion, and nerve pulse propagation, in: *Partial Differential Equations and Related Topics*, in: *Lecture Notes in Math.*, vol. 446, Springer, Berlin, 1975.
- [28] G.F. Gause, *The Struggle for Existence*, Williams and Wilkins, Baltimore, 1935.
- [29] A. Okubo, S. Levin, *Diffusion and Ecological Problems: Modern Perspectives*, Springer, Berlin, 2001.
- [30] S. Aly, I. Kim, D. Sheen, Turing instability for a ratio-dependent predator–prey model with diffusion, *Appl. Math. Comput.* 217 (2011) 7265–7281.
- [31] F. Bartumeus, D. Alonso, J. Catalana, Self-organized spatial structures in a ratio-dependent predator–prey model, *Physica A* 295 (2001) 53–57.
- [32] Y.H. Fan, W.T. Li, Global asymptotic stability of a ratio-dependent predator–prey system with diffusion, *J. Comput. Appl. Math.* 188 (2006) 205–227.
- [33] P.Y.H. Pang, M. Wang, Qualitative analysis of a ratio-dependent predator–prey system with diffusion, *Proc. Roy. Soc. Edinburgh Sect. A* 133 (4) (2003) 919–942.
- [34] W. Wang, Q.X. Liu, Z. Jin, Spatiotemporal complexity of a ratio-dependent predator–prey system, *Phys. Rev. E* 75 (2007) 051913–051921.
- [35] M. Banerjee, Self-replication of spatial patterns in a ratio-dependent predator–prey model, *Math. Comput. Model.* 51 (2010) 44–52.
- [36] M. Banerjee, S. Petrovskii, Self-organised spatial patterns and chaos in a ratio-dependent predator–prey system, *Theor. Ecol.* 4 (2011) 37–53.
- [37] M. Pascual, M. Roj, A. Franc, Simple temporal models for ecological systems with complex spatial patterns, *Ecol. Lett.* 5 (2002) 412–419.
- [38] S. Petrovskii, B.-L. Li, H. Malchow, Transition to chaos can resolve the paradox of enrichment, *Ecol. Complexity* 1 (1) (2004) 37–47.
- [39] W. Wilson, P. Abrams, Coexistence of cycling and dispersing consumer species: Armstrong and McGehee in space, *Am. Nat.* 165 (2) (2005) 193–205.
- [40] M. Baumann, T. Gross, U. Feudel, Instabilities in spatially extended predator–prey systems: spatio-temporal patterns in the neighborhood of Turing–Hopf bifurcations, *J. Theoret. Biol.* 245 (2007) 220–229.
- [41] M. Cross, P. Hohenberg, Pattern formation outside equilibrium, *Rev. Modern Phys.* (65) (1993) 851–1112.
- [42] R. Peng, J. Shi, Non-existence of non-constant positive steady states of two Holling type-II predator–prey systems: strong interaction case, *J. Differential Equations* 247 (2009) 866–886.
- [43] J. Wang, J. Shi, J. Wei, Dynamics and pattern formation in a diffusive predator–prey system with strong Allee effect in prey, *J. Differential Equations* 251 (2011) 1276–1304.
- [44] J. Wu, *Theory and Applications of Partial Functional Differential Equations*, Springer-Verlag, New York, 1996.
- [45] F. Yi, J. Wei, J. Shi, Bifurcation and spatiotemporal patterns in a homogeneous diffusive predator–prey system, *J. Differential Equations* 246 (2009) 1944–1977.
- [46] J. Zhang, W. Li, X. Yan, Hopf bifurcation and Turing instability in spatial homogeneous and inhomogeneous predator–prey models, *Appl. Math. Comput.* 218 (2011) 1883–1893.

- [47] X. Zou, Y. Song, Bifurcation analysis of a diffusive ratio-dependent predator-prey model, *Nonlinear Dyn.* (2014) <http://dx.doi.org/10.1007/s11071-014-1421-2>.
- [48] M. Meixner, A. De Wit, S. Bose, E. Scholl, Generic spatiotemporal dynamics near codimension-two Turing–Hopf bifurcations, *Phys. Rev. E* 55 (3) (1997) 6690–6697.
- [49] L.A.D. Rodrigues, D.C. Mistro, S. Petrovskii, Pattern formation, long-term transients, and the Turing–Hopf bifurcation in a space- and time-discrete predator–prey system, *Bull. Math. Biol.* 73 (2011) 1812–1840.
- [50] A. Rovinsky, M. Menzinger, Interaction of Turing and Hopf bifurcations in chemical systems, *Phys. Rev. A* 46 (3) (1992) 6315–6322.
- [51] T. Faria, Normal forms and Hopf bifurcation for partial differential equations with delay, *Trans. Amer. Math. Soc.* 352 (2000) 2217–2238.
- [52] S.N. Chow, J.K. Hale, *Methods of Bifurcation Theory*, Springer-Verlag, New York, 1982.
- [53] J. Carr, *Applications of Center Manifold Theory*, Springer-Verlag, New York, 1981.
- [54] Yuri A. Kuznetsov, *Elements of Applied Bifurcation Theory*, second ed., Springer Verlag, New York, 1998.
- [55] J. Guckenheimer, P. Holmes, *Nonlinear Oscillations, Dynamical Systems, and Bifurcations of Vector Fields*, Springer-Verlag, New York, 1983.